

CASE INSTITUTE OF TECHNOLOGY
CASE WESTERN RESERVE UNIVERSITY

Publication No. 8102

April 1981

**DEFORMATIONAL SOIL ANISOTROPY:
EXPERIMENTAL EVALUATION AND MATHEMATICAL MODELING**

by

GEORGE GAZETAS

Supported by

The National Science Foundation

Grant No. CME 80-14105

**SOIL MECHANICS RESEARCH LABORATORY
DEPARTMENT OF CIVIL ENGINEERING**

TABLE OF CONTENTS

ACKNOWLEDGEMENT

ABSTRACT

CHAPTER 1 INTRODUCTION

CHAPTER 2 ANISOTROPY IN SANDS

2.1 MICROSCOPIC MANIFESTATION OF SAND ANISOTROPY

2.2 ANISOTROPIC STRESS-STRAIN BEHAVIOR OF SANDS

CHAPTER 3 ANISOTROPY OF CLAYS

3.1 FACTORS INFLUENCING THE ANISOTROPY OF CLAYS

CHAPTER 4 LAYERED/VARVED MEDIA

CHAPTER 5 PHENOMENOLOGICAL DESCRIPTION OF REVERSIBLE DEFORMATION AND YIELDING

5.1 CROSS-ANISOTROPIC ELASTIC STRESS-STRAIN RELATIONS

5.2 ANISOTROPIC YIELDING AND/OR FAILURE CRITERIA

5.3 ANISOTROPIC PLASTIC STRESS-STRAIN RELATIONS

CHAPTER 6 TESTING OF ANISOTROPIC SOILS

6.1 STANDARD TRIAXIAL TESTING

6.2 RESONANT-COLUMN TESTS

6.3 TRUE TRIAXIAL TESTING ON PRISMATIC SPECIMENS

6.4 HOLLOW CYLINDER UNDER AXIAL AND TORSIONAL STRESSES

6.5 IN-SITU MEASUREMENTS

REFERENCES

APPENDIX

ACKNOWLEDGEMENT

This report is based on research supported by a grant
(CME 80-14105) from the National Science Foundation.
This support is kindly acknowledged.

DEFORMATIONAL SOIL ANISOTROPY:
EXPERIMENTAL EVALUATION AND MATHEMATICAL MODELING

ABSTRACT

The causes and nature of anisotropy in sands, clays and varved earthen media is investigated. Based on experimental evidence it is shown that anisotropic mechanical processes, occurring during formation of natural deposits, endow soils with a structure characterized by anisotropic fabric (i.e. with a preferred orientation of particles or particle units) and anisotropic interparticle force systems. As a result, soils exhibit anisotropic deformational characteristics. Upon subsequent straining there tends to occur a reorganization of the initial anisotropic fabric, as particles and particle units tend to achieve a more stable position, with an orientation perpendicular to the direction of the applied maximum stress direction. Therefore, the initial anisotropy of the soil structure tends to be modified in accordance with the anisotropy of the imposed stress system. Whether eventually the soil will bear the anisotropic characteristics of the initial or the applied system depends primarily on the relative size of the forces of each system.

Methods to experimentally determine anisotropic stress-strain and strength characteristics of soils are critically reviewed and the relative merits of various laboratory apparatuses are discussed. Particular emphasis

is finally given to the phenomenological description (mathematical modeling) of both linear reversible (elastic) and nonlinear irreversible (plastic) deformation processes, and some new yielding criteria and hardening rules are reported.

CHAPTER 1

INTRODUCTION

The anisotropic mechanical nature of soils has been known since the early days of development of soil mechanics. For instance, Casagrande & Carillo (1944) talked about shear strength anisotropy in soils and distinguished between *inherent* anisotropy, which is present before the soil is strained and is therefore a physical characteristic of the material, and *induced* anisotropy, which develops 'due exclusively to the strain associated with an applied stress'. In more recent years the anisotropic character of stress-strain behavior of soils has also been recognized (Pickering, 1970). Moreover, attempts have been made to relate anisotropic mechanical behavior to anisotropic fabric and anisotropic interparticle force systems in the soil.

It appears, however, that despite the significant amount of research that has been conducted in many soil laboratories throughout the world, there are still several widespread misconceptions regarding soil anisotropy. For instance, it is frequently claimed that 'soils are not very

anisotropic at small strains but have different behavior near failure for different directions of loading'; in other words, only strength-anisotropy is appreciable. Or it is sometimes argued that strength anisotropy cannot be explained in terms of preferred particle orientation; in other words, anisotropic mechanical behavior is not the manifestation of anisotropic 'structure' of the soil. Moreover, the coefficient of earth pressure at rest, K_o , is often taken as a measure of soil anisotropy; it is then expected that a soil with $K_o = 1$ is less anisotropic (or, perhaps, isotropic) compared to a soil with, say, $K_o = 0.5$.

All these misunderstandings regarding the anisotropy of soils speak of the need for a comprehensive study, based on well-documented experimental facts, of the causes, manifestation and experimental evaluation of soil anisotropy. Such a study has been undertaken and is reported herein.

This report therefore attempts to provide answers to the following questions: What are the causes of anisotropy in soils? How does soil structure^{*} "register" anisotropy? What is the effect of anisotropy on stress-strain-strength behavior of soils? How does an initial anisotropic structure change due to changes in the applied stress-system ('inherent' vs 'induced' anisotropy)? What are the currently employed experimental techniques (in the laboratory and in the field) to measure anisotropic soil characteristics? And finally, how is such mechanical anisotropy modeled for analysis purposes?

* Throughout this report the term soil "structure" is taken to mean the combination of soil "fabric" (which means the orientation and distribution of particles) and interparticle or bonding force systems.

To provide an answer to these questions, the report utilizes published and unpublished experimental evidence regarding the anisotropy of sands (chapter 2), clays (chapter 3) and varved media (chapter 4). Then, chapter 5 presents methods to mathematically model elastic and plastic anisotropic deformation in soils; some of these methods are new in the soil mechanics literature. Finally, chapter 6 critically reviews laboratory and field techniques that are presently used to determine mechanical parameters of anisotropic soils.

CHAPTER 2

ANISOTROPY IN SANDS

Structure anisotropy in sands arises chiefly due to the influence of *gravity* and *grain shape* on the deposition process. Natural granular soils are frequently deposited in approximately horizontal layers under the action of vertical gravity forces imposing one-dimensional deformations. Such anisotropic modes of deposition endow the material with an anisotropic structure. This anisotropy exhibits a vertical axis of rotational symmetry and results in cross-anisotropic (transversally isotropic) deformational characteristics with greater vertical than horizontal stiffnesses.

Laboratory studies of such *inherent anisotropy* in sands have only recently begun following the development of better procedures for undisturbed sampling and special apparatuses for experimental testing (e.g. Arthur et al, 1972). However, indirect evidence of this anisotropy had been provided from full-scale experimental measurements of normal stresses

σ_{zz} and surface settlements of sand deposits subjected to surface loads (Cummings, 1935 ; U.S. Army Corps of Engineers Waterways Experiment Station, 1954). The distribution of σ_{zz} on horizontal planes at various depths showed a larger concentration under the load axis than that predicted by isotropic elasticity; on the other hand, surface settlements away from the loaded area decreased faster than what isotropic elasticity predicted. Both observations can be explained by the cross-anisotropic deformational characteristics of sands which exhibit greater vertical than horizontal stiffness.

In the sequel, experimental evidence of anisotropy in sands is presented. Such evidence comes either from a microscopic examination of the sand structure (including fabric and interparticle forces) or from a phenomenological observation of the response of laboratory sand specimens.

2.1 MICROSCOPIC MANIFESTATION OF SAND ANISOTROPY

Many recent studies have shown that a given cohesionless soil may have different fabrics at the same void ratio or relative density. Characterization of the fabric of cohesionless soils can be done in terms of grain shape factors, grain orientations, and interparticle contact orientations. Furthermore, interparticle contact forces strongly depend on the mechanics of the deposition process in addition to the shape and *grain size distribution*; most grains are not equidimensional but they are at least slightly elongated or tabular.

Preferred Interparticle Contact Orientation

In a gravitational field most of the interparticle contacts have preferred horizontal orientations. These orientations can be described

in terms of the perpendicular directions N_i to the common tangent plane i at the contact point of two grains. The orientation of N_i is defined by the angles α and β measured from the horizontal and vertical axes, respectively, as shown in Fig. 2.1a. Oda (1972 a,b) developed a procedure to determine the angular frequency distributions of the normals $E(\alpha, \beta)$ as a function of α and β . His method involved the use of water-resin solution as pore fluid in samples prepared to a specified void ratio by tapping; after the resin was allowed to harden, thin vertical and horizontal sections of the specimen were cut with a diamond saw and studied by means of a petrographic microscope. For a fabric with an axial symmetry around the vertical axis Z , the frequency $E(\alpha, \beta)$ becomes independent of α . Thus, the distribution of $E(\beta)$ as a function of β can be used to characterize the distribution of interparticle contact normals. Fig. 2.1b portrays such distributions for four sands placed into a cylindrical mold by tapping. The horizontal dashed line represents the distribution for an ideally isotropic fabric. In all cases there is a great proportion of contact plane normals in the near vertical direction. In other words, there exists a marked preferred orientation of the normals towards the direction of deposition.

By considering the projection of interparticle contact areas on three orthogonal planes xy , xz and yz , Oda calculated a fabric index from the distribution of normals $E(\beta)$. Calling S_z , S_y and S_x the summations of all the projected contact areas on the xy , xz and yz planes, respectively, the *anisotropic fabric index* is given by S_z/S_x or S_z/S_y . The preferred orientation of normals translates into:

$$\frac{S_z}{S_x} > 1; \quad S_x = S_y \quad (2.1)$$

This (S_x/S_x) index can be related to the mobilized stress ratio $(\sigma_1/\sigma_3)_{\max}$ and to the dilatancy rate - $dv/d\epsilon_1$ observed during triaxial testing.

It is emphasized that this preferred orientation of interparticle contacts is observed even in sands composed of rounded particles. In fact, Gratton and Fraser (1935) showed that in a random packing of equal spheres most of the tangent planes of interparticle contacts have small-angle dips. This has also been confirmed by the experiments of Kallstenius and Bergau (1961) whereby there was found a greater density of spheres in the vertical than in the horizontal sections.

Preferred Orientation of Long Axes of Particles

Elongated and flat-shaped sandy particles have a strong tendency to adopt a preferential orientation with their maximum dimensions aligned in a horizontal plane, i.e. normal to the direction of deposition. This has been confirmed by numerous investigators (e.g., Parkin, Gerrard & Willoughby, 1968; Lafaber & Willoughby, 1971; Oda, 1972 a,b; Mahmood, 1973). Some of their findings are summarized herein.

Oda presented results of measurements of the orientations of long axes for a large number of grains in the form of frequency histograms such as those of Fig. 2.2b. Particle orientation was characterized by the angle θ with respect to the horizontal (Fig. 2.2a). A sand consisting of particles with an average length-to-width ratio of about 1.65 was placed in a vertical cylindrical mold by tapping its side. In these histograms the orientation of each grain was assigned to one of the 15° intervals between $\theta = -90^\circ$ and $\theta = +90^\circ$. To determine the orientations θ_i , photographic enlargements of thin sections from the resin-impregnated samples were studied. Fig. 2.2b shows the frequency histograms of θ_i

from a vertical section (i.e., a section orientated parallel to the direction of deposition) and a horizontal section (i.e., normal to the axis of deposition). It is evident from this figure that grains of sands formed by tapping have their long axes aligned predominantly in horizontal planes, but symmetrically about the vertical axis.

Parkin, Gerrard & Willoughby (1968) reported results of a similar experimental investigation regarding the fabric of Earlston Sand. Tri-axial specimens were formed by pluvial compaction and impregnated with synthetic resin. Using photographic enlargements of thin vertical and horizontal sections from the specimens, the orientations of the long axes of grains in each section were determined. The relative frequencies of the grain axes were plotted in polar coordinates against the orientation directions using 5° intervals. Shown in Fig. 2.3 are some typical such diagrams; they all reveal a pronounced tendency for particles to adopt a preferred orientation with their maximum dimension lying in the horizontal (H-H) plane, symmetrically about the vertical (V-V) axis. Such a cross-anisotropic fabric is conducive to much greater radial than vertical compressibilities, as discussed in the next section.

The orientations of long axes on a vertical plane from two samples of a well-graded crushed basalt were studied by Mahmood (1973). Frequency diagrams in polar coordinates with 10° intervals are shown in Fig. 2.4. A completely random particle distribution would yield the shown dashed circles. It is evident that samples prepared by pouring exhibit strong preferred orientation of the long grain axes in the horizontal direction; dynamic compaction destroys such a fabric anisotropy, yielding a nearly random fabric.

It is concluded that granular materials deposited under the action of gravity forces develop anisotropic fabrics with a vertical axis of rotational symmetry.

Often, however, naturally occurring sands are deposited under the action of horizontal as well as vertical forces; the resulting fabric exhibits three-dimensional anisotropy having a vertical monoclinic plane of symmetry, as opposed to simple cross-anisotropy having a vertical axis of symmetry. The plane of symmetry contains the line of action of the horizontal force and the long axes of grains are oriented at small dips. For example, in the case of residual soils, a down-hill transportation component, such as creep movement, can influence the fabric anisotropy so that no horizontal plane of material isotropy exists. Similar observations have been made for aeolian deposits: the long axes of the grains concentrate in the direction of the prevailing wind at the time of deposition. This direction defines the vertical plane of monoclinic symmetry. A description of the various types of material symmetry in anisotropic media is given by Gerrard (1977).

Alluvial deposits may also exhibit similar fabric anisotropy. Lafeber & Willoughby (1971) showed that the fabric of a beach sand possesses monoclinic anisotropy with a vertical plane of symmetry normal to the coastline; one of the two long axes of the more or less platy grains tends to align parallel to the coastline while the other dips landward at an angle of about 10° .

The main points of the preceding discussion may be recapitulated as follows:

Under anisotropic stress systems during the formation process, sand grains tend to rest in a preferred most stable position with the number of interparticle contact normals being greatest in the direction of the major principal stress. Also, Their long axes are aligned in a plane perpendicular to the direction of the major principal stress. Consequently, an isotropic (hydrostatic) formation stress system would produce an isotropic fabric, if the fabric is isotropic at the beginning of the process.

2.2 ANISOTROPIC STRESS-STRAIN BEHAVIOR OF SANDS

As a result of their anisotropic fabric, sand specimens invariably exhibit anisotropic deformational characteristics. If they have been deposited under the action of gravity forces alone and subsequently not subjected to other strong non-vertical loads or tectonic deformations, the resulting anisotropy is of the cross-anisotropic type with a vertical axis of rotational symmetry and horizontal planes of isotropy. Experimental evidence of such anisotropic stress-strain behavior is presented below.

A simple way to observe the degree of anisotropy of a sand specimen in the laboratory is by subjecting it to an isotropic (i.e., hydrostatic) loading within a triaxial cell and measuring the axial (ϵ_a), radial (ϵ_r)

and volumetric (ϵ_v) strains. For isotropic materials $\epsilon_1 = \epsilon_r = \frac{1}{3} \epsilon_v$ and any observed deviation from these relationships implies anisotropy. Furthermore, to demonstrate the cross-anisotropic deformational properties of the sample, i.e. to show that the vertical axis is an axis of rotational symmetry, the shape of horizontal cross-sections should be observed during deformation. Any deviation from the circular shape implies lower orders of symmetry, for example triclinic or monoclinic (Gerrard, 1977; Lekhnitskii, 1963), and not cross-anisotropy.

Fig. 2.5 illustrates the anisotropic behavior of a natural sand tested at the University of Tokyo (as referred to by Ladd et al, 1977). Triaxial specimens were obtained from large undisturbed samples, frozen, placed in a triaxial cell, then thawed and finally subjected to a hydrostatic pressure of increasing magnitude. The results reveal a larger (by a factor of about 2.4) compressibility in the horizontal than in the vertical direction, since $\epsilon_v \approx 5.8 \epsilon_v$. Similarly higher horizontal than vertical compressibilities have been observed by El-Sohby & Andrawes (1973) who tested artificial samples of sand in hydrostatic compression. The specimens were prepared in the laboratory by vertically pouring through air or water into a cylindrical mold.

More extreme cases of anisotropic stress-strain behavior have been reported by Kolbuszewski & Jones (1961): for triaxial samples prepared by deposition in air, vertical stiffness under hydrostatic compression was found to be about *five* times the radial stiffness. Furthermore, samples of Earlston Sand prepared by pluvial compaction exhibited vertical stiffness in hydrostatic compression *five* to *six* times higher than the horizontal stiffness (Parkin et al, 1968). The results are portrayed in

Fig. 2.6. Note that a typical distribution of the long axes of grains in selected vertical and horizontal sections of these samples has already been shown in Fig. 2.3; the strong orientation of the fabric is apparent.

A thorough experimental investigation of the anisotropic deformability of loose sands has been recently carried out by Yamada & Ishihara (1979). They performed a series of drained tests on cubical specimens prepared by layered deposition under water. A true triaxial shear test box was employed and the specimens were subjected to a variety of radial stress paths, with the major, intermediate and minor principal stresses oriented independent of the direction of deposition. The results indicate highly cross-anisotropic deformation characteristics "because of the inherent anisotropy of the specimen".

Typical results are summarized in Fig. 2.7 where the three principal strains are plotted as functions of the applied shear to normal octahedral stress ratio, $\tau_{\text{oct}}/p'_{\text{oct}}$. (p'_{oct} remained constant throughout testing.) Fig. 2.7a shows the results of compression (loading) tests; Fig. 2.7b the results of extension (unloading) tests.

In the two compression tests (VC and HC) the specimens were sheared by increasing the major principal stress (in the vertical and horizontal direction, respectively) while decreasing the two minor principal stresses simultaneously; thus the stress conditions were identical in the two tests. The different deformations experienced by the two specimens reveal a pronounced anisotropy: the specimen is stiffest in the direction of deposition. The cross-anisotropic nature of the deformation is also evident: virtually no difference exists between the horizontal lateral strains ϵ_x and ϵ_y in the VC test. However, the vertical and horizontal lateral strains ϵ_z and ϵ_x in the HC test are quite different,

implying, among other things, unequal Poisson's ratios ν_{HV} and ν_{HH} (see Chap. 5). Similar conclusions can be drawn from the results of the two extension tests (VE and HE) portrayed in Fig. 2.7b. Notice also in Fig. 2.8 different volumetric strains experienced during the aforementioned four tests.

A word of caution is appropriate at this point: the fabrics of laboratory prepared samples are most likely to reflect the high order of symmetry usually associated with laboratory formation processes, unlike what actually happens in nature. Extreme care is therefore needed in extrapolating the results of lab tests on artificial samples of field deposits where low orders of symmetry (e.g. triclinic or monoclinic) may be expected. Moreover, detailed measurements of the shape of the deformed cross-sections of triaxial samples are difficult to make, while reported natural fabrics are probably biased towards higher orders of symmetry due to the difficulty in pattern recognition and analysis (Gerrard, 1977). Thus, it is quite difficult to properly assess in the laboratory the particular type of anisotropy of a natural deposit without knowing its geologic history.

Anisotropic Strength

Naturally, fabric anisotropy extends its influence on the strength of granular materials, as has been experimentally demonstrated by Arthur & Menzies (1972), Oda (1972a), Mahmood & Mitchell (1974), Lafeber & Willoughby (1970) and Arthur & Phillips (1975). However, strength anisotropy appears to be much less pronounced than deformational anisotropy. This is most likely the result of *reorganization of the inherent fabric* of the soil under the action of stresses that may be quite high relative to the formation stresses. In other words, usually at failure only remnants of the inherent fabric remain and the fabric is greatly dominated by *stress-induced*

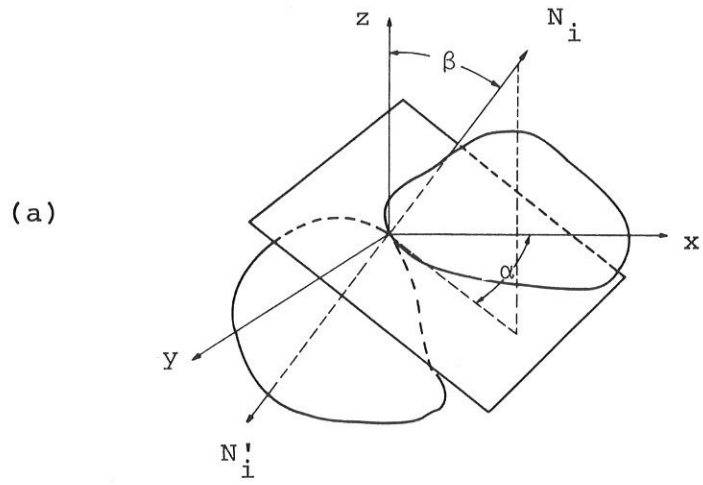
features. The anisotropy of this induced fabric relates primarily to the anisotropy of the applied stress state at failure, although it also reflects (to a lesser degree) the initial (inherent) fabric (see Gerrard, 1977, for a more detailed discussion on induced vs. inherent anisotropy). Thus, conventional triaxial tests on samples formed in a tilting mold so that the angle β varies between the major direction of sand deposition and the direction of major principal stress σ_1 during shear, typically reveal that the highest friction angle occurs at $\beta = 0^\circ$; this angle is only 2° to 4° larger than the lowest friction angle, occurring at $\beta = 90^\circ$ (i.e., when σ_1 acts perpendicular to the direction of formation). Variations in deformational characteristics are more dramatic: vertical moduli larger than the horizontal moduli by a factor of 2 to 5 were measured, apparently because with lower applied stresses the dominant features of the inherent fabric prevail and influence the observed anisotropy.

The validity of this conclusion is demonstrated through Fig. 2.9, obtained from the aforementioned study of Yamada & Ishihara (1979). The figure plots the octahedral stress ratio $\tau_{\text{oct}}/p'_{\text{oct}}$ required to produce either an octahedral strain $\gamma_{\text{oct}} = 1\%$ or failure, as a function of the intermediate principal stress parameter

$$b = \frac{\sigma'_2 - \sigma'_3}{\sigma'_1 - \sigma'_3} \quad (2.2)$$

The results are shown for several radial stress paths; angle θ determines the direction of each path on the octahedral plane: e.g., $\theta = 0^\circ$ for the vertical compression test, $\theta = 120^\circ$ for the horizontal compression test, and so on. It is seen that the stress ratio corresponding to

1% strain decreases as the radial stress path rotates in clockwise direction (θ increases from 0° to 180°). This is attributed to the inherent anisotropy present in the sand specimen. However, failure occurred in the specimen at the same stress ratio independent of whether the test was performed in VC or HC ($\theta = 0^\circ$ or 120°) and VE or HE (180° or 60°). Evidently, "the effects of inherent anisotropy . . . tended to disappear as the stress ratio became large enough to produce maximum volume contraction and failure" (Yamada & Ishihara, 1979).



(b)

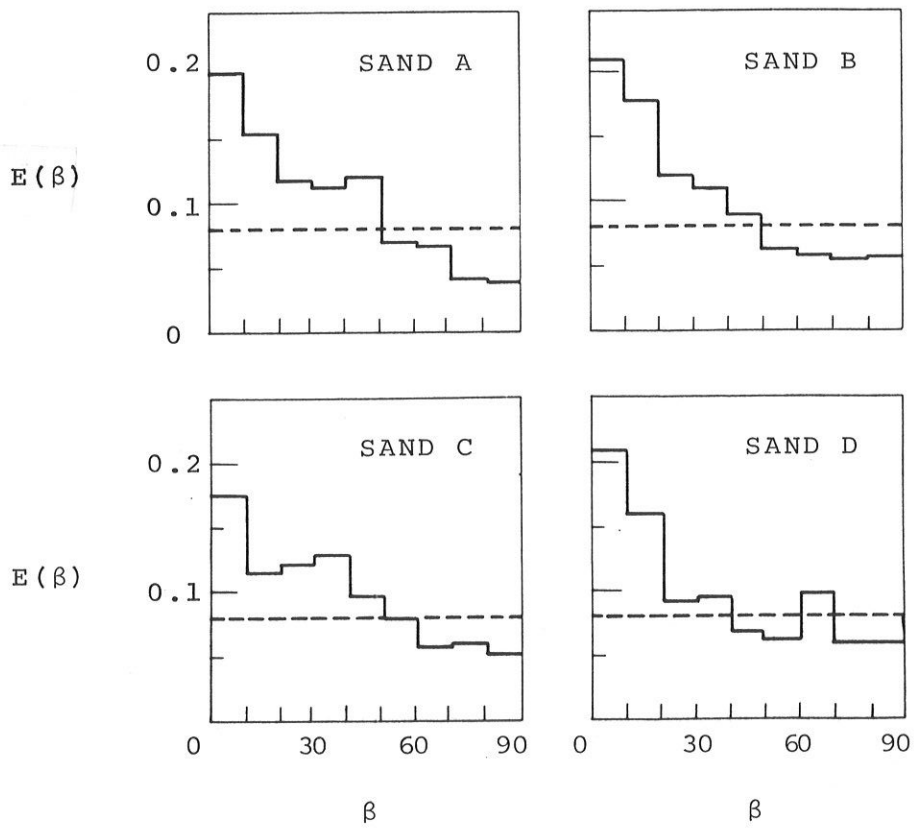
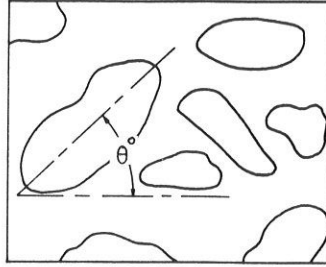


FIG. 2.1 Distribution of interparticle normals in sand (61).

(a)



(b)

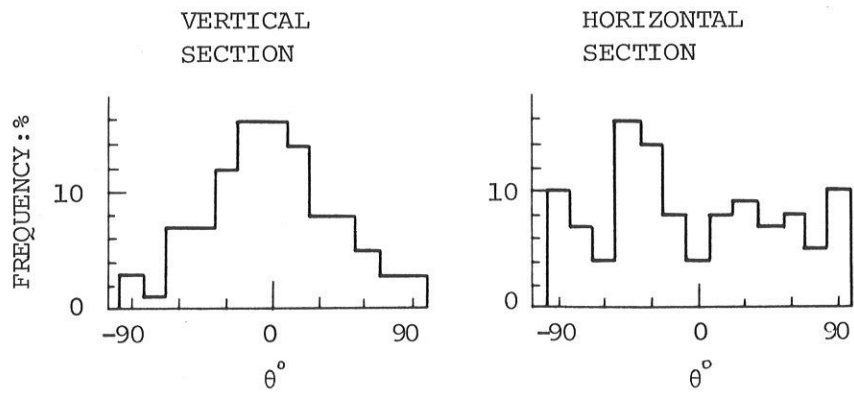
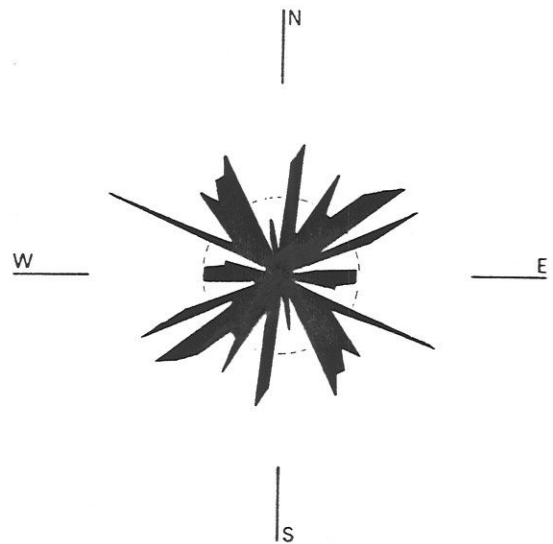
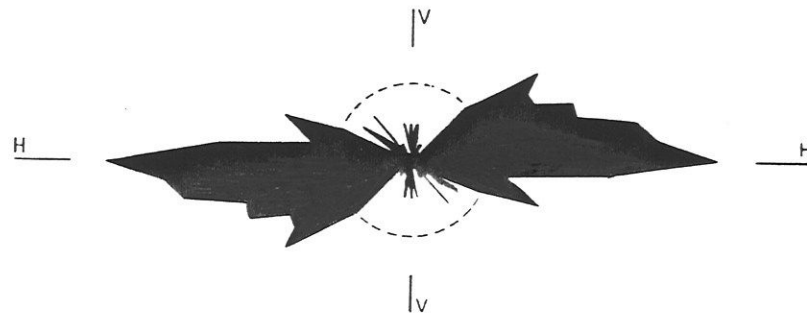


FIG. 2.2 Frequency histograms of long axis orientation in a uniform sand (62).



HORIZONTAL SECTION



VERTICAL SECTION

FIG. 2.3 Relative frequency diagrams of long axes in triaxial specimens of Earlston Sand (27).



FIG. 2.4 Particle orientation diagrams on vertical sections of crushed basalt before and after dynamic compaction (52,53).

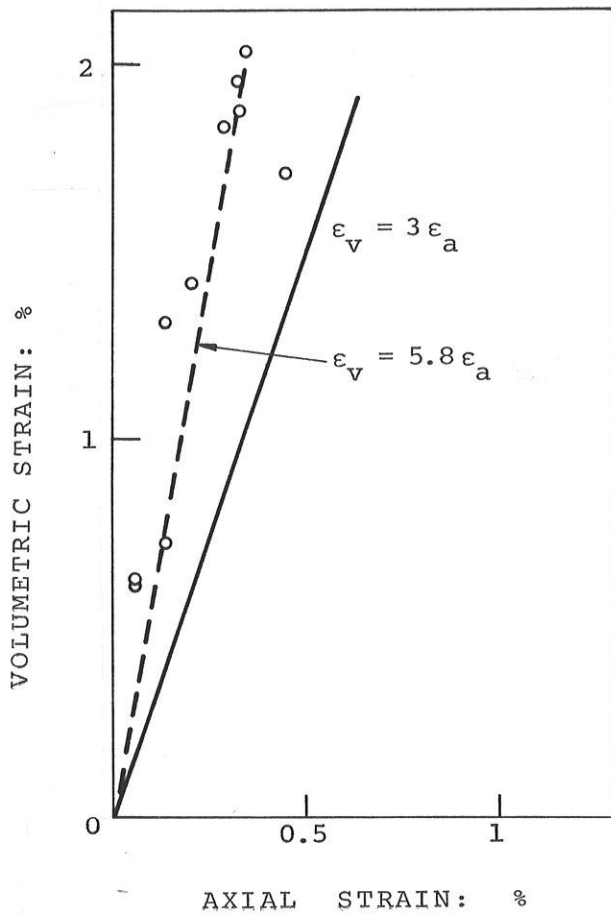


FIG. 2.5

Anisotropic response of Niigata Sand to hydrostatic pressure (44).

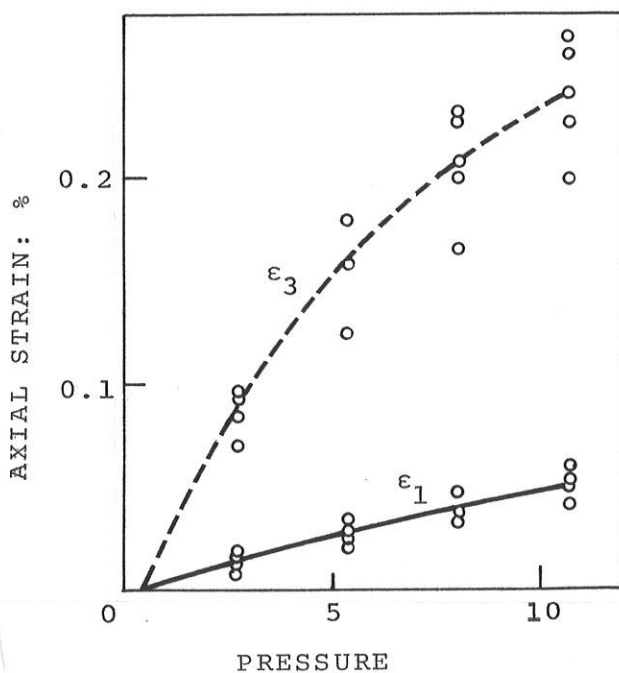


FIG. 2.6

Anisotropic response of Earlston Sand to hydrostatic pressure (64).

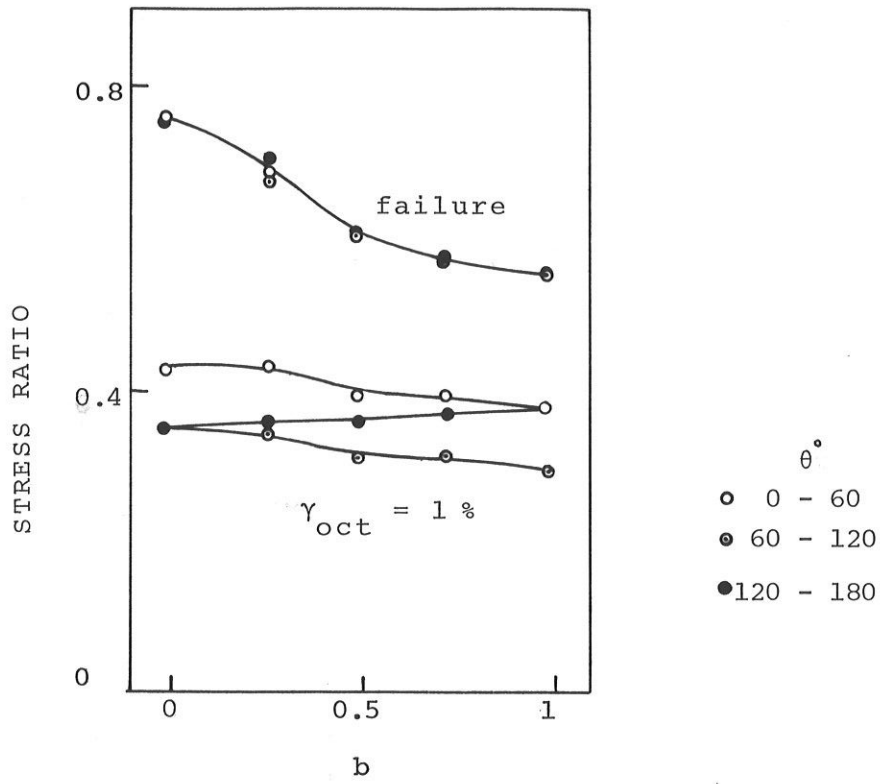


FIG. 2.8 Stress ratio required to cause 1% octahedral shear strain and failure (91).

CHAPTER 3

ANISOTROPY OF CLAYS

Most natural clays are formed under the influence of anisotropic mechanical processes in a variety of physico-chemical environments. As a result, they acquire anisotropic structures: both clay fabric and inter-particle bonds are not random but invariably exhibit some degree of orientation reflecting the characteristics of the formation processes.

As an example, alluvial clay deposits, formed by sedimentation and subsequent one-dimensional consolidation under the action of gravity forces, develop a cross-anisotropic structure characterized by vertical and horizontal principal axes and by lack of orientation on horizontal planes. Microscopic evidence (Lambe, 1958; Martin & Ladd, 1970; Barden, 1971; Kirkpatrick & Rennie, 1973) indicates that fabric anisotropy in such clays primarily takes the form of preferred horizontal orientation of the plate-shaped particles or particle aggregates; their basal planes are aligned in a horizontal direction, normal to the axis of the major principal formation stress.

Structure anisotropy in clays may also arise due to anisotropic electrochemical interparticle bonds, in addition to anisotropic fabric. Perhaps an extreme case of such anisotropy has been observed in the sensitive Canadian Leda Clay (Mitchell, 1970), whose particles and particle aggregates appear to be nearly randomly oriented; yet, highly oriented cementation bonding results in a strongly anisotropic deformational behavior, as discussed later in this chapter.

Cross-anisotropic stress-strain-strength behavior of sedimentary clays is the result of such fabric and bonding anisotropies, i.e., either at the microscale of clay plates or at the macroscale of peds and macropores (Yong, 1971). Considerable attention has been directed towards understanding and measuring clay strength anisotropy (Hansen & Gibson, 1949; Aas, 1965; Lo, 1965; Ward et al, 1965; Duncan & Seed, 1966; Davis & Christian, 1971; Livneh & Greenstein, 1974; etc). Deformational anisotropy has been the subject of relatively fewer studies (Ward et al, 1959, 1965; Kirkpatrick & Rennie, 1973; Saada & Ou, 1973; Atkinson, 1975; Yong & Silvestri, 1979). Yet, there is little doubt that deformational anisotropy is more significant than strength anisotropy (Bazden, 1972). It is, in fact, accepted that the anisotropy of the undrained shear strength results from anisotropy in the pore-pressure-buildup parameter A , which is a deformation parameter, rather than anisotropy of the strength parameters c' and ϕ' .

It is finally noted that macroscopic variations in fabric also produce inherent anisotropy. Characteristic examples are stiff fissured clays and varved clays that are discussed in subsequent sections of this report.

3.1 FACTORS INFLUENCING THE ANISOTROPY OF CLAYS

Little work has been published regarding the factors which affect the type and degree of anisotropy in clays. Since measurements of fabric anisotropy are difficult to make, in most such studies the effects of anisotropic clay structure are inferred from the results of laboratory stress-strain tests on specimens cut at different orientations. Some of the variables that have been found to have a more or less marked influence on the anisotropy of a particular clay are:

- the method of deposition in the field or the method of sample preparation in the laboratory, including the physico-chemical environment;
- the vertical consolidation pressure;
- the apparent overconsolidation due to removal of overburden (unloading), dessication, weathering, etc.;
- changes in the applied stress state ("*induced*" anisotropy);
- the creation or destruction of cementation bonds.

Experimental evidence demonstrating the importance of each of the above factors is presented next.

Method of Sample Preparation

A comprehensive investigation of the sensitivity of one-dimensionally consolidated kaolinite to changes in sample preparation and handling methods has been presented by Martin & Ladd (1970). In preparing the samples, they used different water contents (W) as well as different techniques of placement in the consolidation cylinder. The two extreme types

of preparation procedures are referred to in Table 3.1 as "slurry" and "air dry" clay. "Slurry" is a suspension of saturated clay poured into the consolidation cylinder with water content above the liquid limit. "Air dry" clay, carefully placed in successive one-inch-thick layers in the oedometer, is allowed to gradually absorb water through the bottom porous stone until the entire clay mass becomes moist. Apparently, these two methods of preparation idealize the conditions of natural formation of alluvial and aeolian deposits.

Fabric measurements were made using an x-ray diffraction technique, which is based on the powder method and utilizes wax impregnated samples (Martin, 1966). The technique yields quantitative information concerning the amount and direction of preferred orientation of clay particles. Table 3.1 presents the observed percentage of preferred orientation.

TABLE 3.1 EFFECT OF SAMPLE PREPARATION ON PREFERRED ORIENTATION

<u>Preparation</u>	<u>w% before consolidation</u>	<u>AO%</u>
air-dry	0.7	44
moist clay	20	27
wet-up	100	44
slurry with dispersant	105	76
slurry with flocculant	400	86

(AO) of samples prepared in different ways and consolidated to 1.5 kg/cm^2 . AO may theoretically vary from 0% for an ideally random fabric to 100% for a perfectly oriented fabric. AO has been correlated to the average inclination angle of kaolinite particles or particle clusters via crystallographic theory and experimental measurements. For example, $\text{AO} = 100\%$

corresponds to an average angle of 0° from the horizontal, i.e., to a perfectly horizontal arrangement of particles; $AO = 0\%$ corresponds to an average angle of 45° , implying no preferred orientation of particles (particles at inclinations varying from $0^\circ - 90^\circ$ are met with about equal frequencies).

Table 3.1 indicates that all methods of preparation lead to fabrics that exhibit some degree of orientation; only the "slurry" samples, however, are strongly oriented with the basal planes of particles and particle-clusters nearly perpendicular to the direction of the major principal stress. Extrapolating to natural clays, alluvial deposits are more likely to be anisotropic than aeolian or residual soils. It should be noted though, that at higher consolidation pressures the AO of all samples increases, as discussed below.

1-Dimensional Consolidation Pressure

As repeatedly mentioned in the preceding text, one-dimensional consolidation, with its anisotropic deformation and stress condition, is the primary cause of anisotropy in soils. Naturally, therefore, by increasing the major consolidation stress $\sigma_1' = \sigma_v'$ one expects an increase in the amount of orientation, with the particles and particle-aggregates assuming an increasingly horizontal arrangement.

This expectation is indeed confirmed by Fig. 3.1, in which the measured AO of kaolinite samples is plotted as a function of σ_v' (Martin & Ladd, 1970). It is noticed that changes in fabric under increasing consolidation stress are most pronounced in samples that initially have a nearly random orientation and least pronounced in relatively well oriented samples.

The greatest degree of orientation achieved by one-dimensional consolidation of kaolinite by Martin & Ladd, 1970, is 92%, which corresponds to an average inclination of about 8° .

An indirect evidence of the importance of consolidation pressure on soil anisotropy is offered by the published experimental testing data on London Clay (Ward et al, 1965; Skempton & Henkel, 1957; Bishop et al, 1965): as noticed by Gibson, 1974, "there is a slight tendency for the ratio of horizontal to vertical moduli to increase with depth" despite the simultaneous decrease of the overconsolidation ratio (see discussion on following section).

The author is not aware of any other systematic investigations on the influence of consolidation stress on the fabric or the stress-strain behavior of natural and artificial clays.

Apparent Overconsolidation

Overconsolidation in natural soil deposits may either arise directly from the removal of overburden due, for example, to erosion and melting, or maybe the apparent outcome of dessication and weathering. The latter inflicts primarily sedimentary deposits after their first exposure to the atmosphere during a period of geologic uplift or change in climatic conditions.

There is ample evidence suggesting that clay anisotropy is strongly influenced by increasing overconsolidation. This is due to the resulting macroscopic fabric changes which primarily take the form of strong patterns of *fissures* developing parallel to the bedding direction. For instance, Fookes & Denness (1969) found major sets of such fissures in a variety of

cretaceous sediments. Fabric patterns of the joints and fissures in the heavily overconsolidated London Clay have been found and reported, among others, by Skempton et al (1969) and Rowe (1972). It appears that such fissures and joints, mostly parallel to the bedding direction, are at least to some extent associated with the relatively high compressive stresses in the horizontal direction caused by the overconsolidation process (Gerrard, 1977; Brooker & Ireland, 1965).

As a consequence, with increasing overconsolidation ratio (OCR) the degree of anisotropy in clays increases; the horizontal modulus is, in general, considerably higher than the vertical modulus in heavily overconsolidated clays, contrary to what is happening in sands. Normally consolidated clays, on the other hand, usually exhibit milder degrees of anisotropy with the moduli ratio E_H/E_V being either larger or smaller than 1.

The highly overconsolidated London Clay offers the best documented evidence of markedly anisotropic mechanical characteristics in naturally formed soils. Being a marine deposit of the Eocene age, London Clay has an almost uniform mineralogy with illite and montmorillonite as major components, kaolinite and chlorite as minor ones (Gilkes, 1968). It has been heavily overconsolidated due to the removal of 200 m to 400 m overburden caused by erosion and melting (Skempton & Henkel, 1957; Bishop et al, 1965). Its fabric exhibits anisotropy both at the microscale (particle clusters aligned with their flat faces perpendicular to the direction of consolidation) and the macroscale (strong pattern of fissures and joints mostly aligned in the horizontal direction).

The mechanical properties of London Clay have been measured by Ward and his colleagues at the Building Research Station (1959, 1965). They performed undrained compression tests on undisturbed cylindrical samples cut with their axis vertical, horizontal or inclined at 45° to the vertical. Simons (1971) reported the results of drained triaxial tests and Atkinson (1975) of undrained and drained triaxial and plane-strain tests with a variety of stress paths. Typical results are summarized in Table 3.2. Note that the reported shear moduli G_{VH} have not been measured in the laboratory but theoretically back-figured from the undrained Young's modulus of the 45° inclined samples by Gibson (1974). As it has been pointed out by Pagano and Halpin (1968) and Saada (1968), these determined

TABLE 3.2 TYPICAL ANISOTROPIC PROPERTIES OF LONDON CLAY

Sample location	Test	E_H/E_V	ν_{VH}	ν_{HH}	G_{VH}/E_V
average of 8 sites	UU, CIUC	1.60	0.50	0.20	--
Ashford	UU, CIUC	1.84	0.50	0.08	0.38
"	" "	2.00	0.50	0.20	0.40
Barbican Arts Centre	CIUC	1.20	0.50	0.40	--
" " "	CIDC	2.00	0.19	0.00	0.536
" " "	CID PSC	1.94	--	--	--
Typical upper bound	CIDC	2.50	0.00	-0.35	0.77

UU = (undrained) unconfined compression test

CIUC and CIDC = undrained and drained, respectively, triaxial compression test on isotropically consolidated samples

CIDPSC = drained plane-strain compression test on isotropically consolidated sample

values of G_{VH} are likely to be erroneous because of incorrect estimation of E_{45° . Extraneous bending and shearing end effects are generated whenever samples cut with their axis inclined to the vertical are tested in triaxial compression. Thus the obtained E_{45° values may under- or over-estimate the actual modulus. A detailed analysis and discussion of this problem is presented in Chapter 5 of this report.

It may be seen in Table 3.2 that horizontal moduli larger than the vertical moduli by a factor of about 2 is rather the rule in London Clay. It is noted in passing that the undrained unconfined shear strength is also greater in the horizontal direction (S_{uh}) than in the vertical direction (S_{uv}), but only by a factor of about 1.5, compared with the factor of 2.0 pertaining to stiffness.

A typical set of drained stress-strain relations of London Clay from the Barbican Arts Centre reproduced from Atkinson (1975) is shown in Fig. 3.2. Both cylindrical (CIDC) and plane-strain (CIDPSC) compressive stress-strain and tangent modulus-strain curves are portrayed in this figure.

Dessication - The effect of natural dessication of clay sediments was simulated in the laboratory by allowing saturated samples of consolidated kaolin to dry by evaporation to water contents below the shrinkage limit (Franklin & Mattson, 1972). The samples were initially prepared from a kaolin-water slurry under one-dimensional consolidation pressures ranging from 80 to 400 psi, with two distinct stress histories. A series of direction P-wave velocity measurements on prismatic samples with water contents below and above the shrinkage limit were then carried out. Typical results are given in Fig. 3.3. It is seen that

the velocities are always higher in the horizontal (V_H) than the vertical (V_V) direction.

At initial moisture contents the average velocity ratio V_H/V_V is only about 1.05, but it dramatically increases upon drying, as soon as the water content drops below the shrinkage limit. With continued drying below this limit the velocity ratio approaches a nearly constant value. Final velocity ratio values in air-dry samples varied from 1.34 to 2.02, being generally higher for higher consolidation pressures. Recalling that

$$\frac{E_H}{E_V} \approx \left(\frac{V_H}{V_V} \right)^2 \quad (3.1)$$

it is concluded that apparent overconsolidation due to drying of one-dimensionally consolidated kaolinitic clays, appreciably increases fabric anisotropy and may lead to horizontal moduli values of up to 1.80 to 4.20 times the vertical moduli values.

Overconsolidated kaolinite - Not every strongly overconsolidated clay is characterized by an E_H/E_V ratio greater than 1. An example is kaolinite overconsolidated by removal of the overburden (one-dimensional unloading). Fig. 3.4, for instance, plots typical stress-strain relations from CIU tests on kaolinite samples with an OCR of about 8 (Gazetas & Botsis, 1981). The samples were cut vertically or horizontally from consolidated ($\sigma'_v \approx 100$ psi) kaolin-water slurry. Notice that E_H/E_V as well as S_{uh}/S_{uv} are less than 1, i.e. the clay is stiffer and stronger in the direction of consolidation. Very similar results for kaolinite have been reported by Bhaskaran (1975).

Nonetheless, as the OCR increases both E_H/E_V (compression) and S_{uh}/S_{uv} (compression) increase, and both can become greater than 1 at high OCR values. Moreover, E_H/E_V from extension tests has been found to be greater than unity for all values of OCR (Gazetas & Botsis, 1981; Saada & Ou, 1973; Parry & Nadarajah, 1974). Both of the above aspects can be attributed to the tendency of developing fissures parallel to the bedding, during unloading in a perpendicular direction. (Gerrard, 1977).

Changes in Applied Stress System

It is well recognized that the mechanical behavior of soils depends not only on the (imposed) current state of stress but, also, on the whole "*stress history*" since formation of the deposit; stress history exerts its main influence by modifying the fabric and the interparticle forces in the clay soil. Consequently, changes in the effective stresses applied to clays usually produce a fabric reorganization and, in certain cases, alter the interparticle bonds so that the type and degree of pre-existing (often called inherent) anisotropy change.

As a general rule, the anisotropic structure produced by a deviatoric stress of a given orientation (e.g., one-dimensional consolidation following deposition) will be modified by the application of a deviatoric stress system of different orientation, so that the resultant fabric becomes more resistant and stable against the applied stress tensor. Therefore, the resultant fabric exhibits to some degree the anisotropy and symmetries of all the stress systems that have been applied throughout its history; the stronger of these stress systems will most likely have the greatest influence on the final structure. For instance, the stress induced anisotropy of initially isotropic clays assumes the same planes of symmetry as

those induced by the applied stress tensor; whereas, an initially highly oriented clay (e.g. London Clay) will retain its (inherent) anisotropy against applied stress systems of the size usually encountered in engineering practice. Significant fabric reorientation in such cases would take place as a result of shear failure, well after the peak effective stress ratio has been reached (e.g., during a triaxial test). Indeed, polarizing microscope observations made on thin sections from plane-strain test samples of K_0 -consolidated kaolin (Barden, 1972) reveal only a slight degree of clay plate alignment in the inclined failure zone at the peak effective stress ratio (i.e., at axial strains of about 4.5%); such an alignment becomes high only after the large shearing displacements associated with the residual state and the formation of a visible Coulomb slip plane.

Along the same lines, the aforementioned study by Martin & Ladd (1970) on the factors affecting the fabric of K_0 -consolidated kaolin resulted in the following: although changes in the direction of the major applied stress (e.g. by rotating the direction of one-dimensional consolidation) do alter the direction of preferred orientation, very large stress changes are necessary to produce significant changes in the fabric.

Cementation Bonds

The existence of a preferentially oriented system of interparticle cementation bonds in a clay may create a strongly anisotropic structure, although the clay fabric exhibits only a slight orientation. Such appears to be the case with the normally consolidated sensitive Canadian clay, known as Leda Clay (Soderman & Quigley, 1965; Quigley & Thompson, 1966;

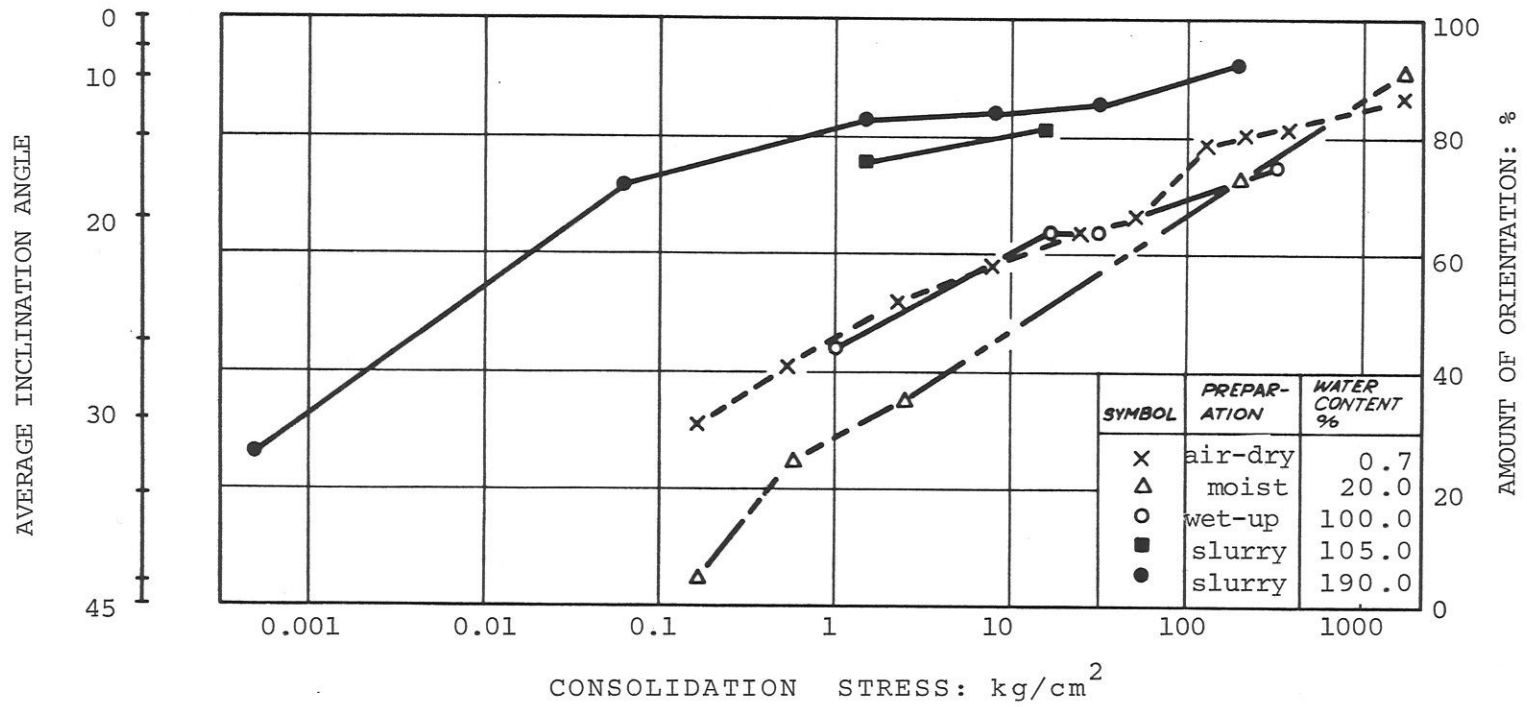
Mitchell, 1970, 1972; LaRochelle & Lefebvre, 1971; Yong & Silvestri, 1979). Microscopic examinations have established the "open, flocculated arrangement of particles and the strong [oriented] cementation bonds at inter-particles contacts" (Yong & Silvestri, 1979).

As a result, the behavior of such a structure can be summarized as follows:

1. At low confining pressures, i.e. at pressures that are not sufficiently high to cause a breakdown of cementation bonds, Leda Clay behaves as a cross-anisotropic nearly elastic material; the vertical Young's modulus is larger than the horizontal modulus by a factor of about 1.70, as it can be seen from the stress-strain unconfined compression test curves shown in Fig. 3.5 (Yong & al, 1979).

2. At higher pressures the bonds are progressively destroyed and the clay exhibits brittle behavioral characteristics; marked strength anisotropy is observed during drained tests, being primarily attributed to the preferred orientation of the cementation bonding (Mitchel, 1970). In contrast, most (uncemented) normally consolidated clays show only a minor anisotropy associated with the drained strength parameters c' and ϕ' ; undrained strength anisotropy is mainly due to the anisotropy of the pore pressure parameter A_f , which is a deformation parameter.

FIG. 3.1 Dependence of particle orientation in a normally-consolidated Kaolin upon the vertical consolidation stress (54).



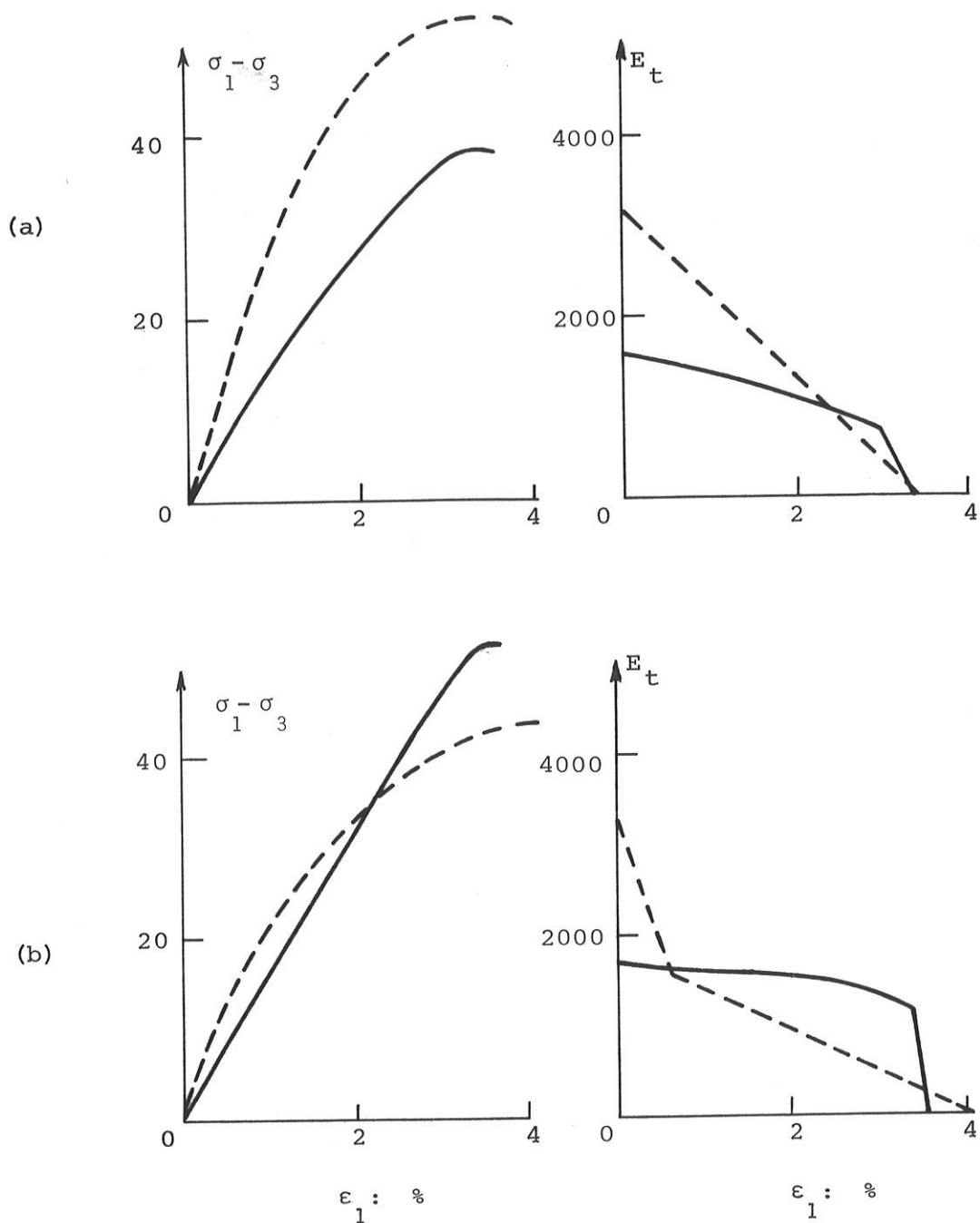


FIG. 3.2 Deformational behavior of London Clay (4):
 (a) standard triaxial test; (b) plane-strain test
 (stresses are in psi)

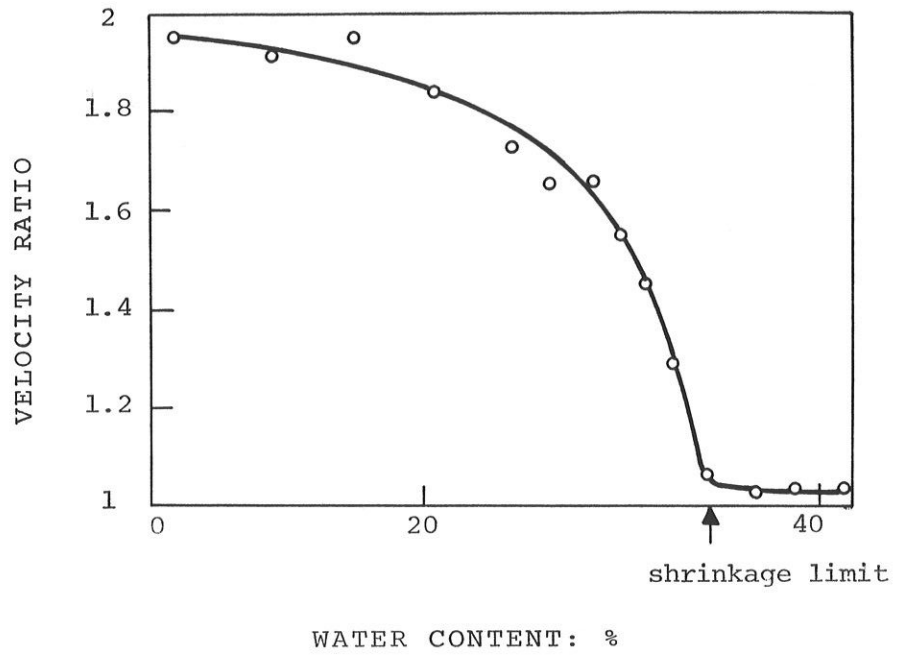


FIG. 3.3 Effect of decreasing water content on directional velocity ratio of Kaolin (22)

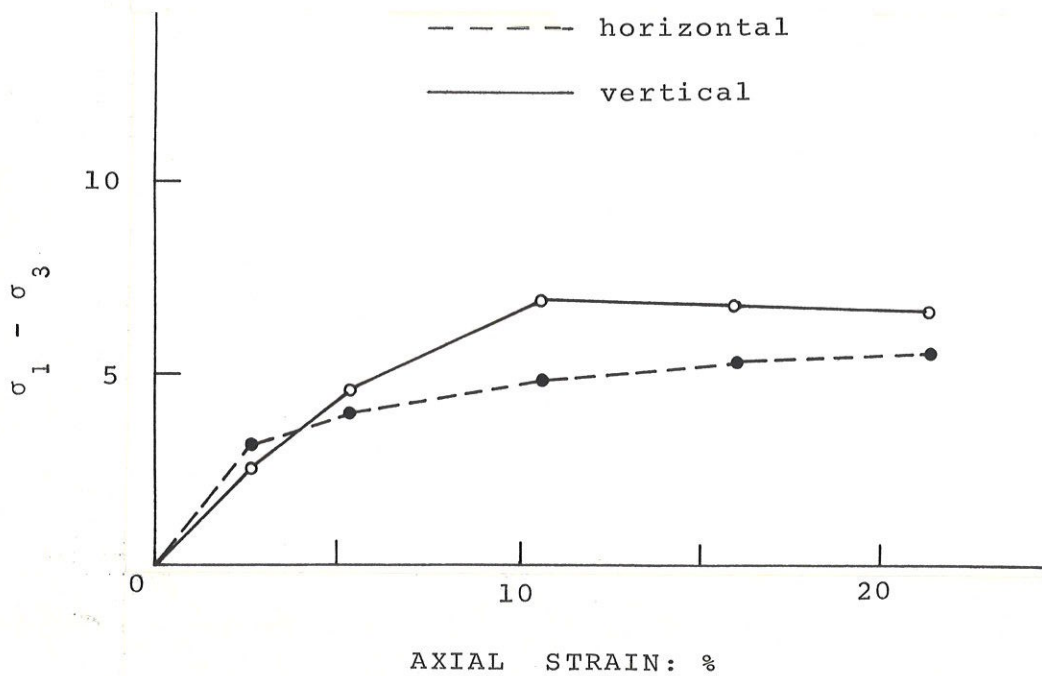
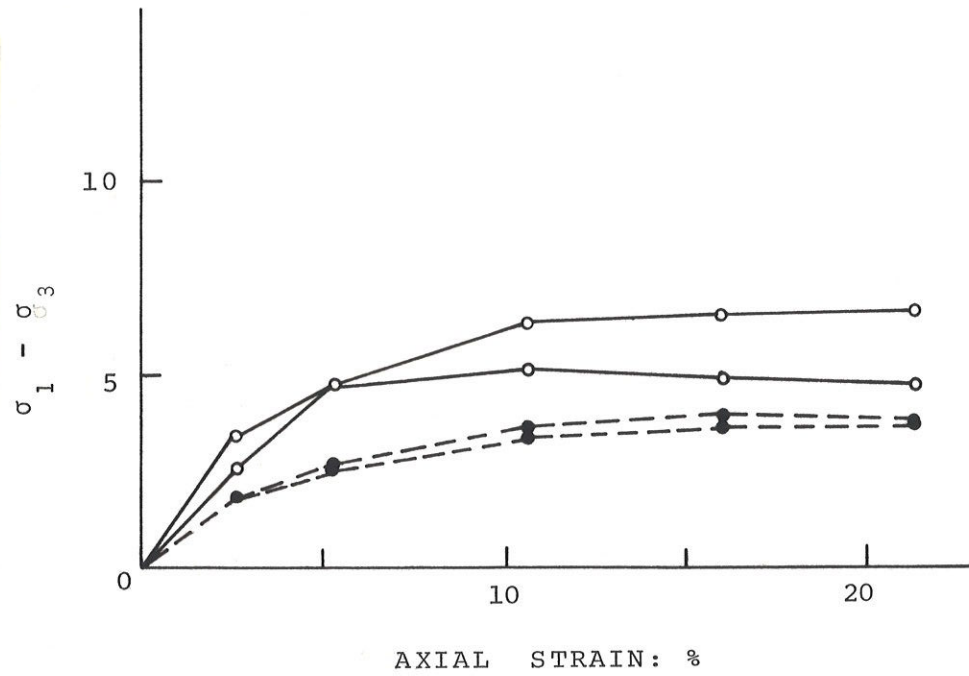


FIG. 3.4 Stress-strain behavior of overconsolidated Kaolinite (25). (stresses are in psi)

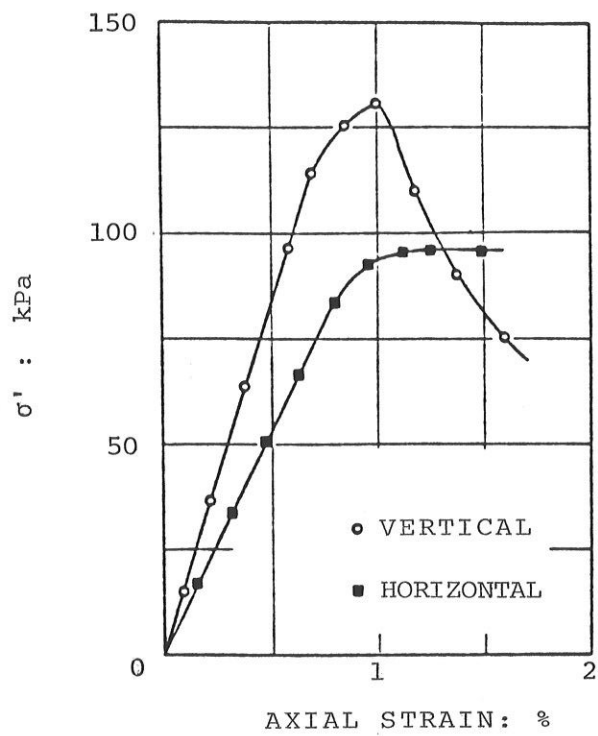


FIG. 3.5 Unconfined compression stress-strain curves for Leda Clay (94).

CHAPTER 4

LAYERED/VARVED MEDIA

In geotechnical practice one often encounters soil and rock masses consisting of numerous relatively thin layers bounded by parallel planes and with varying material properties and thicknesses in the direction normal to the bounding planes. Typical examples are varved clays, reinforced earth and regularly jointed rocks.

It has been theoretically established (Brekhoviskikh, 1960; Salamon, 1968) that, when certain restrictions are met, the "bulk" mechanical behavior of a layered varved medium is the same with the behavior of an *'equivalent' homogeneous cross-anisotropic* material. This is true even if the individual layers/varves consist of isotropic material. The following conditions should be fulfilled so that such a similarity in behavior can be considered:

a) all interface planes between layers remain in contact and are fully continuous in the sense that no relative displacement occurs;

b) the thickness and elastic properties of the layers vary randomly in the direction perpendicular to the parallel bounding planes of the layers;

c) a representative sample of the stratified mass, on the basis of which the 'equivalent homogeneous' properties are evaluated, must contain a "large enough" number of layers; and

d) the length of such a representative sample must be much smaller than a 'characteristic' loading dimension of the problem (e.g. the radius of a circular foundation, etc.).

Under these conditions, the cross-anisotropic elastic constants of the homogeneous medium, which is 'equivalent' to a system of n isotropic layers of total length L , are (see chapter 6 for the precise meaning of each constant):

$$\nu_{HH} = \frac{\sum_1^n \left(\frac{t_i \nu_i E_i}{1 - \nu_i^2} \right)}{\sum_1^n \left(\frac{t_i E_i}{1 - \nu_i^2} \right)} \quad (4.1)$$

$$\nu_{HV} = (1 - \nu_{HH}) \frac{\sum_1^n \left(\frac{t_i \nu_i}{1 - \nu_i} \right)}{\sum_1^n \left(\frac{t_i E_i}{1 - \nu_i^2} \right)} \quad (4.2)$$

$$E_H = (1 - \nu_{HH}^2) \frac{\sum_1^n \left(\frac{t_i E_i}{1 - \nu_i^2} \right)}{\sum_1^n \left(\frac{t_i E_i}{1 - \nu_i^2} \right)} \quad (4.3)$$

$$E_V = \left\{ \frac{\sum_1^n \left(\frac{t_i}{G_i} \frac{1 - 2\nu_i}{2(1 - \nu_i)} \right)}{\sum_1^n \left(\frac{t_i E_i}{1 - \nu_i^2} \right)} + \frac{2 \nu_{HV}^2}{(1 - \nu_{HH}) E_H} \right\}^{-1} \quad (4.4)$$

$$G_{HH} = \frac{\sum_1^n (t_i G_i)}{\sum_1^n (t_i G_i)} \quad (4.5)$$

$$G_{VH} = \left\{ \sum_{i=1}^n (t_i G_i^{-1}) \right\}^{-1} \quad (4.6)$$

in which V and H denote directions perpendicular and parallel to the bounding planes, respectively; E_i , G_i and ν_i are the elastic constants of varve i with a relative thickness t_i given by

$$t_i = \frac{T_i}{L}; \quad \sum_{i=1}^n t_i = 1 \quad (4.7)$$

where T_i is the thickness of this varve. Certain restrictions must be satisfied by these equivalent cross-anisotropic elastic constants due to the thermodynamic requirement of non-negative strain energy function under all possible states of stress (see Salamon, 1968; Wardle & Gerrard, 1972; and also Pickering, 1970). The most significant of these restrictions pertains to the ratio of shear moduli:

$$\frac{G_{HH}}{G_{VH}} \geq 1 \quad (4.8)$$

that is, the shear modulus (G_{HH}) in planes parallel to the direction of stratification is larger than the shear modulus (G_{VH}) in planes normal to it. This relation is confirmed by a range of experimental measurements on earthen materials, conducted by Gerrard et al, 1972.

The restriction on Poisson's ratio ν_{HH} is

$$-1 \leq \nu_{HH} \leq 1/2 \quad (4.9)$$

i.e., differs from the restriction for a general cross-anisotropic material only in the upper limit (see Chap. 6). Poisson's ratio ν_{HV} , on the other hand, satisfied the following inequalities:

$$-1 \leq \nu_{VH} \leq 2 \quad (4.10)$$

with the upper limit being approached in the case of an ideal reinforced earth material, as shown by Harrison & Gerrard, 1972.

A special case of interest is the one where all layers (varves) are *incompressible*, e.g. due to undrained loading conditions. Poisson's ratios in all individual varves are equal to $\nu_i = 1/2$, and the equivalent cross-anisotropic constants reduce to:

$$\nu_{HH} = \nu_{VH} = \nu_{HV} = 1/2$$

$$E_V = E_H \quad (4.11)$$

$$G_{VH} < G_{HH} = E_H/3$$

Note that the material anisotropy is reflected in the inequality of Eq. 4.11. Apparently if all varves have the same shear modulus, then $G_{VH} = G_{HH} = G$ and the bulk material behaves in an isotropic manner.

It is of interest to briefly discuss the degree to which several earthen materials satisfy the criteria of the aforementioned "equivalence".

Varved Clay

Varved clays are rhythmically banded sediments, formed by cyclic deposition in glacial lakes, during the ice-retreat stage. Each varve is composed of alternating layers of light-colored summer-deposited silt and dark winter-deposited clay. Usually, the thickness of the varve does not exceed 1 inch, while the composition and properties of the clay and silt layers are quite variable. This variability depends not only on the geologic conditions of deposition but on the subsequent stress history, as well. Extensive deposits of varved clay are encountered in the northern US, Canada and Europe. Fig. 4.2 is a photograph of a typical vertical section through a varved clay.

It is not difficult to see that a varved clay would respond to stresses as a cross-anisotropic homogeneous material. Indeed, all the aforementioned conditions required for such an 'equivalence' are satisfied with reasonable accuracy by most varved clays: 1) the interface planes are parallel to each other, usually in the horizontal direction; 2) due to a formation process by a more or less continuous deposition, no slippage is likely to occur at the layer interfaces^{*}; 3) the thickness and elastic properties of the varves and layers show only small and apparently random variability with depth (i.e normal to the interfaces); 4) finally, the thickness of the varve is very small (usually $T \leq 1$ inch) much larger than the anticipated characteristic dimension in most geotechnical applications.

* in fact, there is no distinct interface, in the mathematical sense of the term, but rather a transition zone with silt "grading" into clay.

In addition, it is noted that especially the clay layers are likely to exhibit strong preferred orientation parallel to the interface planes of the varves, as photometric measurements have showed (Mitchell, 1976).

Reinforced Earth

Vidal (1969) first proposed that soft soils should be reinforced in critical directions by thin sheets or strips of a stiffer material. The resulting composite material, reinforced earth, has improved mechanical properties and has, thus, been extensively used in retaining walls, quay walls, dam or cofferdam works, rafts, foundations, highway or airport pavements and other geotechnical structures. The reinforcement may consist of circular bars, thin strips, or meshes of metal, wire or plastic; the use of flexible sheets of synthetic fabric has also been rapidly increased especially in the construction of embankments and pavements on soft clayey soils (Yamanouchi, 1970).

In all types of reinforced earth the reinforcing layers are extremely thin and have very large in-plane (or axial) stiffness relative to the soft soil layers. Moreover, the reinforcing layers are closely spaced relative to the critical loading dimensions for most practical problems. If the spacing of the layers does not follow any systematic pattern but, as is often the case, remains more or less constant away from the loading area, all aforementioned conditions for 'equivalence' are fulfilled. Therefore, *sheet* reinforced earth behaves as a homogeneous *cross-anisotropic* material and *rod or strip* reinforced earth behaves

as a homogeneous *orthorhombic* material (Brekhoviskikh, 1960; Salamon, 1968). The latter exhibits a lower order of symmetry than a cross-anisotropic material; it possesses three mutually perpendicular planes of symmetry, e.g. a plane containing a layer of reinforcement, a normal plane parallel and symmetrical with respect to the reinforcement and a normal plane perpendicular to the reinforcement.

The equivalent cross-anisotropic material constants of sheet reinforced earth have been derived from the more general equations (4.1) to (4.6) by Harrison & Gerrard (1972). They are presented below for easy reference. Considering a distance L perpendicular to the direction of layers, calling S the combined thickness of the reinforcing layers, s the corresponding relative thickness ($s = S/L$), and denoting with a subscript r the constants of the reinforcing material, the cross-anisotropic constants are:

$$\nu_{HH} = \left(\frac{(1-s)E\nu}{1-\nu^2} + \frac{sE_r\nu_r}{1-\nu_r^2} \right) / \left(\frac{(1-s)E}{1-\nu^2} + \frac{sE_r}{1-\nu_r^2} \right) \quad (4.12)$$

$$\nu_{HV} = (1-\nu_{HH}) \left(\frac{(1-s)\nu}{1-\nu} + \frac{s\nu_r}{1-\nu_r^2} \right) \quad (4.13)$$

$$E_H = (1-\nu_{HH})^2 \left(\frac{(1-s)E}{1-\nu^2} + \frac{sE_r}{1-\nu_r^2} \right) \quad (4.14)$$

$$E_V = \left\{ \frac{1-s}{E} \left(1 - \frac{2\nu^2}{1-\nu}\right) + \frac{s}{E_r} \left(1 - \frac{2\nu_r^2}{1-\nu_r}\right) + \frac{2\nu_{HV}^2}{(1-\nu_{HH})E_V} \right\}^{-1} \quad (4.15)$$

$$G_{HH} = E_H / (2(1+\nu_{HH})) \quad (4,16)$$

$$G_{VH} = \left\{ \frac{2(1-s)(1+\nu)}{E} + \frac{2s(1+\nu_r)}{E_r} \right\}^{-1} \quad (4,17)$$

in which E , ν are the constants of the soft soil assumed to be isotropic. Simpler formulas pertaining to particular limiting cases of reinforced earth materials have been derived by Harrison & Gerrard, 1972.

Regularly Jointed Rock

Large natural rock masses are often broken by fracture surfaces which are classified as joints or faults* and can have a significant effect on the gross mechanical response (Jaeger & Cook, 1969). Commonly, joints occur in sets of regularly spaced, more or less parallel, planes with a variety of orientations. Major joint sets can extend for miles with joint spacing ranging from inches to several feet.

The presence of joints may affect the behavior of rock masses in two ways: first, irreversible joint slip may occur at high shear traction levels; second, the pre-slip deformation and stress field is influenced by the normal and tangential stiffnesses, as well as the spacing, of the joints. When the length scales ("characteristic" dimensions) of interest are large compared with the joint spacing and the relative displacements across joints are reversible (linearly related to joint tractions) and small compared to joint spacing, the jointed rock mass exhibits

* the distinction into joints and faults is purely geological and does not have any effect on the bulk behavior of a rock mass.

the bulk deformational characteristics of a continuous homogeneous cross-anisotropic material (Morland, 1976). Any axis perpendicular to the joint planes is an axis of rotational material symmetry while on planes parallel to joints the material properties are the same in all directions (planes of isotropy).

The degree of anisotropy depends primarily on the ratios of the "gross" joint moduli (Λ_s and Λ_d) to the elastic shear and Young's moduli of the rock (G and E). Morland (1976) has presented the bulk stress-strain relations for such a jointed rock mass. From these relations one can readily deduce the equivalent cross-anisotropic elastic constants:

$$E_V = E / (1 + E/\Lambda_d) \quad (4.18)$$

$$G_{VH} = G / (1 + G/\Lambda_s)$$

$$E_H = E \quad (4.20)$$

$$\nu_{HH} = \nu \quad (4.21)$$

$$\nu_{VH} = \nu \frac{E_V}{E} \quad (4.22)$$

in which E , G and ν are the Young's modulus, shear modulus and Poisson's ratio of the intact part of the rock, respectively; Λ_s and Λ_d are the "gross" shear and normal joint moduli, obtained from the shear and normal stiffnesses of each joint, λ_s and λ_d :

$$\Lambda_s = \lambda_s T, \quad \Lambda_d = \lambda_d T \quad (4.23)$$

where T is the average spacing between the joints.

It is evident from Eqs. (4.18) - (4.22) that there are only *four* independent anisotropic material constants, namely, E , G , Λ_s and Λ_d . In contrast, a general cross-anisotropic elastic material needs five independent deformation constants to be fully described, as discussed in the following chapter.

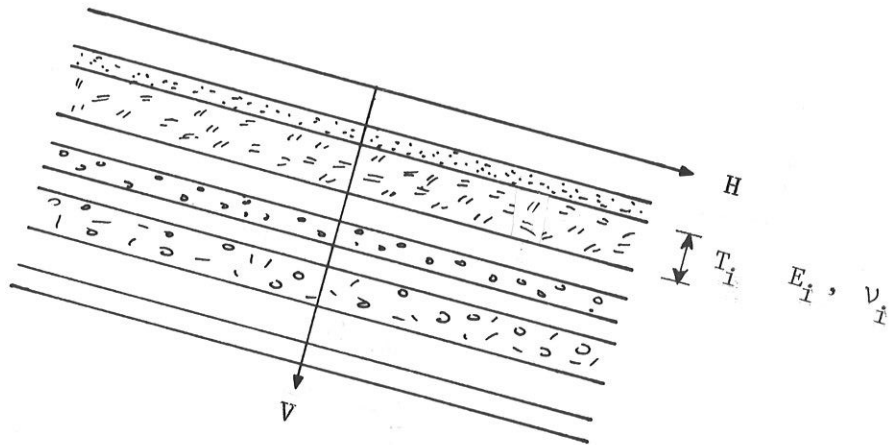


FIG. 4.1 Geometry of layered system

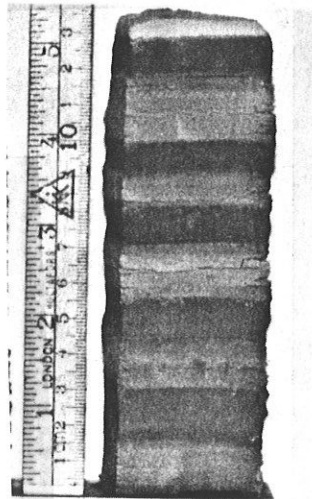


FIG. 4.2 Typical vertical section through a varved clay (59)

CHAPTER 5

PHENOMENOLOGICAL DESCRIPTION OF REVERSIBLE
DEFORMATION AND YIELDING

Soils, in general, are *particulate* multiphase materials, composed of isolated or aggregated solid particles, fluid and gas. In principle, two different approaches may be adopted to determine the mechanical properties of such complex materials: the *microscopic/mechanistic approach* and the *phenomenological approach*. The former attempts to relate the mechanical behavior of a mass of soil to the properties and physical-chemical interactions among the individual soil particles and the fluid and gas phases. This requires a detailed knowledge of the arrangement, shape and properties of the individual particles; thus, it is rather intractable at present, despite several worthwhile studies that have been published in recent years (Rowe, 1962; De Josselin de Jong, 1971; Spencer, 1964; Bazant, Ozaydin & Krizek, 1975; David & Deresiewicz, 1977; Mehrabadi, Nemat-Nasser & Oda, 1980). Probabilistic theory appears to offer the proper framework for this approach.

The phenomenological approach, on the other hand, treats the locally heterogeneous soil as a continuum. A mathematical model is used to correlate the external mechanical excitation to the resulting material responses, without necessarily explaining the mechanisms which lead to these responses. This approach is used herein to study the response of soils with oriented structure by treating them as homogeneous and cross-anisotropic continua.

It is convenient to distinguish two different types of response of a continuum to applied stresses: one associated with small and reversible deformations and another with large deformations that are, at least partly, irreversible. Linear elasticity has been traditionally used to model the first type of response, while nonlinear elastoplastic models are necessary to describe the mechanical behavior of the second type.

5.1 CROSS-ANISOTROPIC ELASTIC STRESS-STRAIN RELATIONS

In the sequel, it is assumed without loss of generality that the vertical axis z is the axis of rotational material symmetry and the axes x and y define the horizontal planes of isotropy. It has been shown (Love, 1892) that an elastic material with this type of anisotropy (usually called "*cross-anisotropy*" or "*transverse isotropy*") is characterized by the following independent elastic constants: two Young's moduli E_H and E_V in the horizontal and vertical direction, respectively; two Poisson's ratios ν_{VH} and ν_{HH} relating lateral horizontal strain to imposed vertical or horizontal strain, respectively; and one

shear modulus G_{VH} controlling the distortion of a vertical element with sides parallel to the z and x (or y) axes. Fig. 5.1 schematically illustrates the meaning of each independent material constant.

With the system of coordinate axes (x,y,z) coinciding with the principal material axes, the generalized Hooke's Law reads

$$\epsilon_{ij} = S_{ijkl} \sigma_{kl} \quad (5.1)$$

where S_{ijkl} is the fourth-rank compliance tensor. Eq. (5.1) can be explicitly stated in matrix form as follows:

$$\begin{Bmatrix} \epsilon_{xx} \\ \epsilon_{yy} \\ \epsilon_{zz} \\ \epsilon_{xy} \\ \epsilon_{xz} \\ \epsilon_{yz} \end{Bmatrix} = \begin{bmatrix} \frac{1}{E_H} & -\frac{\nu_{HH}}{E_H} & -\frac{\nu_{VH}}{E_V} & 0 & 0 & 0 \\ -\frac{\nu_{HH}}{E_H} & \frac{1}{E_H} & -\frac{\nu_{VH}}{E_V} & 0 & 0 & 0 \\ -\frac{\nu_{HV}}{E_H} & -\frac{\nu_{HV}}{E_H} & \frac{1}{E_V} & 0 & 0 & 0 \\ 0 & 0 & 0 & \frac{1}{2G_{HH}} & 0 & 0 \\ 0 & 0 & 0 & 0 & \frac{1}{2G_{VH}} & 0 \\ 0 & 0 & 0 & 0 & 0 & \frac{1}{2G_{VH}} \end{bmatrix} \begin{Bmatrix} \sigma_{xx} \\ \sigma_{yy} \\ \sigma_{zz} \\ \tau_{xy} \\ \tau_{xz} \\ \tau_{yz} \end{Bmatrix} \quad (5.2)$$

As Eq. (5.2) stands, there are seven compliance parameters. However, since the strain energy density function

$$W = \frac{1}{2} S_{ijkl} \sigma_{ij} \sigma_{kl} \quad (5.3)$$

remains non-negative for all possible states of stress, one may deduce that

$$S_{ijkl} = S_{klij} \quad (5.4)$$

For the compliance tensor of Eq. (5.2), the above relation yields

$$\frac{\nu_{VH}}{E_V} = \frac{\nu_{HV}}{E_H} \quad (5.5)$$

Further, due to the condition of isotropy on horizontal planes,

$$G_{HH} = \frac{E_H}{2(1+\nu_{HH})} \quad (5.6)$$

Thus, there remain only five independent material constants in Eq. (5.2)

Moreover, the aforementioned thermodynamic argument of non-negative strain energy leads to the following inequalities which restrict the range of values of the material constants (Hearmon, 1961; Pickering, 1970; Gibson, 1974):

$$E_V, E_H, G_{VH} \geq 0 \quad (5.7)$$

$$-1 \leq \nu_{HH} \leq 1 - 2n\nu_{VH}^2 \quad (5.8)$$

in which

$$n = E_H/E_V \quad (5.9)$$

Incompressible Material

Geotechnical engineers are often concerned with predicting stresses and deformations in water-saturated clays. Immediately after the application of external loads, saturated clays behave as incompressible materials. This is due to the very small permeability of clays and the relative incompressibility of water, compared to that of the porous clayey structure. The special relations that the compliance parameters of such materials satisfy [in addition to obeying (5.5) - (5.9)] can be obtained by examining the expression relating volumetric strain to stresses. From (5.2)

$$\begin{aligned}\epsilon_{\text{vol}} &= \epsilon_{\text{xx}} + \epsilon_{\text{yy}} + \epsilon_{\text{zz}} \\ &= (1-n\nu_{\text{VH}}-\nu_{\text{HH}}) \frac{\sigma_{\text{xx}}}{E_{\text{H}}} + n(1-2n\nu_{\text{VH}}) \frac{\sigma_{\text{yy}}}{E_{\text{H}}} + (1-n\nu_{\text{VH}}-\nu_{\text{HH}}) \frac{\sigma_{\text{zz}}}{E_{\text{H}}}\end{aligned}\quad (5.10)$$

Incompressibility requires that $\epsilon_{\text{vol}} \equiv 0$, which leads to

$$\nu_{\text{VH}} = \frac{1}{2} \quad (5.11a)$$

$$\nu_{\text{HH}} = 1 - \frac{1}{2} n \quad (5.11b)$$

Furthermore, the condition of non-negative strain energy requires that

$$0 \leq n \leq 4 \quad (5.12)$$

which replaces the more general inequalities (5.8). It is noted that at the upper limit, $n = 4$, the strain energy function vanishes identically (i.e. for all conceivable applied stress systems). Consequently,

the material becomes absolutely rigid and no deformations occur under applied loads. (Gibson, 1974; Gazetas, 1981).

Rotation of Coordinate Axes

The elements of the compliance tensor S_{ijkl} of an anisotropic body depend on the direction of the axes of the coordinate system. It is of interest to know how these compliance constants relate when expressed in two different coordinate systems.

In general, for a system of axes (x', y', z') which do not coincide with the principal material axes (x, y, z) , the stress-strain relations may be expressed as

$$\epsilon'_{ij} = S'_{ijkl} s'_{kl} \quad (5.13)$$

where

$$S'_{ijkl} = \begin{bmatrix} S'_{1111} & S'_{1122} & S'_{1133} & S'_{1112} & S'_{1113} & S'_{1123} \\ & S'_{2222} & S'_{2233} & S'_{2212} & S'_{2213} & S'_{2223} \\ & & S'_{3333} & S'_{3312} & S'_{3313} & S'_{3323} \\ & \text{symm.} & & S'_{1212} & S'_{1213} & S'_{1223} \\ & & & & S'_{1313} & S'_{1323} \\ & & & & & S'_{2323} \end{bmatrix} \quad (5.13a)$$

Let the position of the (x', y', z') system be defined by the direction cosines a_{ij} ($i, j = 1, 2, 3$) with respect to the principal material system (x, y, z) , where $a_{11} = \cos(x', x)$, $a_{12} = \cos(x', y)$, . . . , $a_{23} = \cos(y', z)$, . . . , and so on. The transformation of the compliance tensor then takes the form:

$$S'_{ijkl} = a_{im} a_{jn} a_{ko} a_{lp} S_{mnop} \quad (5.14)$$

Of particular interest in many applications is the special case of a coordinate system obtained by rotating the principal coordinate system about one of its axes, say y , as shown in Fig. 5.2. Calling ϕ the angle (z, z') and introducing the "technical constants" E_V , E_H , ν_{VH} , ν_{HH} and G_{VH} , Eq. (5.14) leads to the following formulas:

$$S'_{1111} = \frac{\cos^4 \phi}{E_H} + \frac{\sin^4 \phi}{E_V} + \left(\frac{1}{G_{VH}} - \frac{2\nu_{VH}}{E_V} \right) \cos^2 \phi \sin^2 \phi \quad (5.15a)$$

$$S'_{2222} = \frac{1}{E_H} \quad (5.15b)$$

$$S'_{3333} = \frac{\sin^4 \phi}{E_H} + \frac{\cos^4 \phi}{E_V} + \left(\frac{1}{G_{VH}} - \frac{2\nu_{VH}}{E_V} \right) \cos^2 \phi \sin^2 \phi \quad (5.15c)$$

$$S'_{1122} = - \left(\frac{\nu_{HH}}{E_H} \cos^2 \phi + \frac{\nu_{VH}}{E_V} \sin^2 \phi \right) \quad (5.15d)$$

$$S'_{2233} = - \left(\frac{\nu_{VH}}{E_V} \cos^2 \phi + \frac{\nu_{HH}}{E_H} \sin^2 \phi \right) \quad (5.15e)$$

$$S'_{1133} = \left(\frac{1}{E_H} + \frac{1}{E_V} + \frac{2\nu_{VH}}{E_V} - \frac{1}{G_{VH}} \right) \sin^2 \phi \cos^2 \phi - \frac{\nu_{VH}}{E_V} \quad (5.15f)$$

$$S'_{1212} = \frac{\cos^2 \phi}{G_{HH}} + \frac{\sin^2 \phi}{G_{VH}} \quad (5.15g)$$

$$S'_{1313} = \left(\frac{1}{E_V} + \frac{1}{E_H} + \frac{2v_{VH}}{E_V} - \frac{1}{G_{VH}} \right) \sin^2 \phi + \frac{1}{G_{VH}} \quad (5.15h)$$

$$S'_{2323} = \frac{\cos^2 \phi}{G_{VH}} + \frac{\sin^2 \phi}{G_{HH}} \quad (5.15i)$$

$$S'_{2213} = \left(\frac{v_{HH}}{E_H} - \frac{v_{VH}}{E_V} \right) \sin 2\phi \quad (5.15j)$$

$$S'_{1213} = \left(\frac{1}{G_{VH}} - \frac{1}{G_{HH}} \right) \frac{\sin 2\phi}{2} \quad (5.15k)$$

$$S'_{3313} = \left\{ 2 \left(\frac{\cos^2 \phi}{E_V} - \frac{\sin^2 \phi}{E_H} \right) - \left(\frac{1}{G_{VH}} - \frac{2v_{VH}}{E_V} \right) \cos 2\phi \right\} \frac{\sin 2\phi}{2} \quad (5.15l)$$

$$S'_{1123} = S'_{2223} = S'_{3323} = S'_{2312} = 0 \quad (5.15m)$$

$$S'_{1113} = S'_{2213} = S'_{3313} = S'_{1312} = 0$$

On the basis of the above relations the following *invariants of transformation* may be deduced:

$$I_1 = S'_{1111} + S'_{3333} + 2S'_{1133} = \frac{1}{E_V} + \frac{1}{E_H} - \frac{2v_{VH}}{E_V} \quad (5.16a)$$

$$I_2 = S'_{1313} - 4S'_{1133} = \frac{1}{G_{VH}} + \frac{4v_{VH}}{E_V} \quad (5.16b)$$

$$I_3 = S'_{1212} + S'_{2323} = \frac{1}{G_{VH}} + \frac{1}{G_{HH}} \quad (5.16c)$$

$$I_4 = S'_{1122} + S'_{3322} = -\frac{\nu_{VH}}{E_V} - \frac{\nu_{HH}}{E_H} \quad (5.16d)$$

Eqs. (5.15) and (5.16) are very useful when studying the behavior of anisotropic bodies under stress systems whose principal axes do not coincide with the principal material axes. Such cases are discussed in Chapter 6, in connection with triaxial testing of anisotropic soils.

5.2 ANISOTROPIC YIELDING AND/OR FAILURE CRITERIA

"Yielding" and "failure" may be interpreted as the occurrence of *irreversible* deformations or of any definable *discontinuity* in the material response to stresses. A phenomenological yielding (failure) criterion may be established with or without the aid of a mathematical model. If extensive experimental measurements are made in all components of the stress space, the need for theoretical modeling becomes secondary; the occurrence of yielding (failure) can be tabulated either in numerical or graphical form. But such a purely empirical approach is, of course, very costly. A mathematical model can considerably facilitate the determination of yielding (failure) by reducing the number of experimental measurements to that required for the determination of a few key parameters.

In order to be acceptable, a yielding (failure) criterion must:

- (1) be independent of the choice of coordinate axes; (2) have only one

root for any radial loading path; (3) be mathematically operational; and (4) lead to unambiguous definition of the principal yielding directions. Next, some of the most prominent yielding criteria for anisotropic media are briefly presented and their relevance to modeling yielding of soils is discussed.

Hill Criterion

The criterion proposed by Hill (1950) for the yielding of anisotropic materials may be written as

$$\begin{aligned}
 & F(\sigma_{yy} - \sigma_{zz})^2 + G(\sigma_{zz} - \sigma_{xx})^2 + H(\sigma_{xx} - \sigma_{yy})^2 \\
 & + 2L\tau_{yz}^2 + 2M\tau_{zx}^2 + 2N\tau_{xy}^2 - 1 = 0
 \end{aligned} \tag{5.17}$$

where F, G, H, L, M, N = parameters characteristic of the current state of anisotropy.

For a cross-anisotropic material with a vertical axis of symmetry Eq. (5.17) simplifies to

$$\begin{aligned}
 & F[(\sigma_{yy} - \sigma_{zz})^2 + (\sigma_{zz} - \sigma_{xx})^2] + H(\sigma_{xx} - \sigma_{yy})^2 \\
 & + 2L(\tau_{yz}^2 + \tau_{xz}^2) + 2(F + 2H)\tau_{xy}^2 - 1 = 0
 \end{aligned} \tag{5.18}$$

Furthermore Eq. (5.18) reduces to the Von Mises's criterion if no anisotropy exists. The material parameters with respect to the principal axis of anisotropy, are obtained from the uniaxial yield stresses X, Y

and Z, in compression, and R, S and T, in shear. In the case of cross-anisotropic yielding $X = Y$, $R = S$ and the appropriate relations are:

$$X^{-2} = F + H, \quad Z^{-2} = 2F, \quad R^{-2} = 2L \quad (5.19)$$

Two are the main limitations of Hill's criterion when it is applied to soils: (1) it assumes that hydrostatic stresses have absolutely no effect on yielding; and (2) it implies that the material is equally sensitive to extension and compression. Nonetheless, it is possible to develop extended forms of Hill's criterion to partly account for material sensitivity to hydrostatic stresses and for any differences in extension and compression. This was done by Yong & Silvestri (1979) in their study of Leda Clay. They found such an extended Hill's criterion very appropriate for modeling the brittle failure of this sensitive clay. However, it is evident that different modifications of Eq. (5.18) are needed for each particular material. This severely limits the applicability of the criterion to model yield and failure of soils.

A final note is deemed appropriate. Hill's model is an extension of Von Mises' isotropic yield criterion which is related to the amount of energy that is used to distort rather than change the volume of a body. Since in anisotropic materials distortion can not be separated from dilatation, Eqs. (5.17) and (5.18) are not related to distortional energy.

Davis-Christian Undrained Strength Criterion

A similar criterion, proposed by Davis & Christian (1971) as a

strength criterion for saturated clays subjected to undrained loading, takes the form:

$$\left(\frac{\sigma_{zz} - s_{uV}}{2} - \frac{\sigma_{xx} - s_{uH}}{2} \right)^2 + \tau_{xz}^2 \frac{s_{u45}^2}{s_{uV}s_{uH}} = \left(\frac{s_{uV} + s_{uH}}{2} \right)^2 \quad (5.20)$$

where s_{uV} , s_{uH} and s_{u45} are the undrained strengths for a vertical, horizontal and inclined at 45° to the vertical compressive loading.

The main advantage of Eq. 5.20 as an undrained failure criterion lies in its simplicity. It has been used by its proponents to derive simple expressions for bearing capacity of strip footings, assuming rigid-perfectly plastic soil behavior (slip-line analysis). Moreover, it is in reasonable agreement with experimentally measured compressive strengths, $s_{u\theta}$, at various orientations θ .

Note, however, that it is basically a plane-stress criterion as it ignores the influence of the off-plane stress components σ_{yy} , τ_{xy} and τ_{zy} . Thus, its use even for plane-strain problems can at best be considered as an approximation. Furthermore, it does not account for different strengths in extension and compression loading, and its performance under complex stress paths has not been established. Finally, accurate determination of s_{u45} from a standard triaxial compression test is questionable due to extraneous shear and bending boundary effects that are generated, as will be discussed in detail in Section 6.1.

Gol'denblat-Kopnov Criterion

To improve the inadequacies of the preceding criteria the number of terms in the yield function should increase so that all stress components are represented and linear terms (in addition to quadratic) are also included. Such a criterion has been proposed by Gol'denblat & Kopnov (1968, 1971).

For cross-anisotropic materials with a vertical axis of symmetry, (z) the criterion takes the form

$$\begin{aligned}
 & [P(\sigma_{xx} + \sigma_{yy}) + R \sigma_{zz}]^\alpha + [F(\sigma_{xx}^2 + \sigma_{yy}^2) + H \sigma_{zz}^2 \\
 & + J(\sigma_{xx}\sigma_{zz} + \sigma_{yy}\sigma_{zz}) + I \sigma_{xx}\sigma_{yy} + 2M(\tau_{xz}^2 + \tau_{yz}^2) + 2N \tau_{xy}^2]^\beta \\
 & - 1 = 0
 \end{aligned} \tag{5.21}$$

where the exponents are usually taken as

$$\alpha = 1, \quad \beta = 1/2$$

The 'strength' constants P, R, F, H, J, I, M and N are experimentally determined. Notice that for pressure insensitive isotropic materials with identical behavior in tension and compression Eq. (5.21) reduces to the form of the von Mises yield criterion.

Saada & Ou (1973) established the validity of Eq. (5.21) with three different clays tested in a hollow-cylinder apparatus under combination of hydrostatic, axial and torsional stresses. The main drawback of this criterion, as pointed out by Wu (1974), is the "mixing of linear

and quadratic coefficients and subsequent confusion in physically linking the model parameters to engineering strengths". The reader is referred to Wu (1974) for an elaborate discussion on this point.

Tsai-Wu Stress Tensor Polynomial Criterion

An operationally simple yield criterion for anisotropic materials has been proposed by Tsai & Wu (1971) in the form of a scalar function of two *strength tensors*:

$$f(\sigma_{ij}) = F_{ij} \sigma_{ij} + F_{ijkl} \sigma_{ij} \sigma_{kl} - 1 = 0 \quad (5.22)$$

$$i, j, k, l = 1, 2, 3$$

wherein F_{ij} and F_{ijkl} are strength tensors of the second and fourth rank, respectively.

Using contracted stress notation, Eq. (5.22) may be written as

$$F_i \sigma_i + F_{ij} \sigma_i \sigma_j - 1 = 0 \quad (5.22a)$$

$$i, j = 1, 2, \dots, 6$$

An interesting feature of Eq. (5.22) is that the elements of the stress yield tensors F_i and F_{ij} can be expressed in terms of engineering yield measurements from uniaxial and multiaxial tests. For instance,

$$\begin{aligned}
 F_1 &= \frac{1}{X_t} - \frac{1}{X_c} \\
 F_2 &= \frac{1}{Y_t} - \frac{1}{Y_c} \\
 &\dots \dots \dots \\
 F_6 &= \frac{1}{S_{yz}} - \frac{1}{S_{zy}}
 \end{aligned}
 \tag{5.23}$$

where X_t , X_c , Y_t , Y_c , . . . are the uniaxial extension and compression strengths in the x and y direction, respectively; S_{yz} and S_{zy} are the positive and negative shear strengths with respect to the x plane, as schematically shown in Fig. 5.3. Note that for anisotropic materials with different moduli in extension and compression $|S_{yz}| \neq |S_{zy}|$ in coordinates other than the principal material directions.

For a cross-anisotropic material under plane-stress conditions (5.22) simplifies to

$$F_1 \sigma_1 + F_2 \sigma_2 + F_6 \sigma_{12} + F_{11} \sigma_1^2 + F_{22} \sigma_2^2 + F_{66} \sigma_{12}^2 + 2F_{12} \sigma_1 \sigma_2 - 1 = 0
 \tag{5.24}$$

Eq. (5.24) represents an ellipsoid in the 3-dimensional stress space (σ_1 , σ_2 , σ_{12}). Note that the coefficients of all terms (except F_{12}) can be determined from uniaxial tests. The term involving F_{12} represents the interaction between normal stresses in the 1 and 2 directions. A biaxial test is apparently needed to evaluate F_{12} . For example a biaxial extension test with $\sigma_1 = \sigma_2 = \sigma$ and all other stresses equal to zero would lead to

$$(F_{11} + F_{22} + 2F_{12}) \sigma^2 + (F_1 + F_2) \sigma - 1 = 0 \quad (5.25)$$

from which F_{12} is readily obtained.

Wu (1974) has shown that the Stress Tensor Polynomial Yield Criterion is the most general of all currently available criteria. It can readily be specialized to account for different material symmetries, multi-dimensional space, and multiaxial stress. Its applicability to soils, however, has not yet been explored. Research is currently underway at Case Institute of Technology to establish the validity of this criterion in modeling yield and failure of overconsolidated clays.

5.3 ANISOTROPIC PLASTIC STRESS-STRAIN RELATIONS

To model the elastoplastic deformational behavior of soils one needs: (1) an appropriate "*flow*" rule which relates the increments of plastic strain to the applied stress tensor, once a yield surface has been reached; and (2) a "*hardening*" rule which describes the modification of the initial yield criterion (yield surface) in the process of plastic deformation.

The most frequently used flow rule is the so-called "*associative*" or "*normality*" rule, which states that the plastic strain increments are proportional to the gradient of the yield criterion:

$$d \epsilon_{ij}^p = \lambda \frac{\partial f(\sigma_{ij})}{\partial \sigma_{ij}} \quad (5.26)$$

in which λ is a proportionality constant and $f(\sigma_{ij})$ is the yield function. The normality rule implies that if the principal plastic strain increments

$d \epsilon_i^p$, $i = 1, 2, 3$, are plotted on a set of axes coinciding with the principal stress axes σ_i , $i = 1, 2, 3$, the vector resultant of the plastic strain increment $d \epsilon_i^p$, will be directed in the outward normal to the yield surface $f(\sigma_i)$.

Several studies have shown that the "normality" rule is a reasonable approximation for many soils, at least well before (ultimate) failure is reached (Yong, 1971; Yamada & Ishihara, 1979; etc.). Thus, "normality" is at present widely used in soil mechanics. Some researchers, however, have questioned its validity and proposed non-associative flow rules, where a plastic potential function $g(\sigma_{ij})$ is substituted for $f(\sigma_{ij})$ in (5.26) (Lade, 1972). Further experimental studies are needed before definitive conclusions can be drawn.

Three types of hardening rules are presently used:

(1) '*Isotropic*' hardening, which assumes that the initial yield surface expands isotropically, retaining its original shape and orientation in the g -dimensional stress space. Such a rule accounts neither for the Bauschinger effect nor for the dependence of soil characteristics on direction, as plastic deformation occurs.

(2) '*Kinematic*' hardening, whereby the initial yield surface retains both its size and shape, but is allowed to translate in the stress space. This rule somewhat overestimates the Bauschinger effect and can cover only certain particular cases of plastic anisotropy.

(3) *Combined 'kinematic' and 'isotropic'* hardening, whereby the yield surface changes in size and translates at the same time. Such rules may realistically model the Bauschinger effect and, to a certain extent, stress induced anisotropy.

A new '*anisotropic*' hardening rule, originally proposed by Baltov & Sawczuk (1965), has been recently implemented by Botsis & Gazetas (1981) to develop elastoplastic undrained stress-strain relations for saturated overconsolidated clays. Motivated by the Stress-Tensor-Polynomial Yield Criterion, the new rule can take the following dimensionless form:

$$N_{ijkl} (S_{ij} - \beta_{ij}) (S_{kl} - \beta_{kl}) - 1 = 0 \quad (5.27)$$

with

$$S_{ij} = \sigma_{ij} - \frac{1}{3} \sigma_{kk} \delta_{ij} \quad (5.27a)$$

where S_{ij} is the deviatoric stress tensor, β_{ij} denotes the tensor of total translation in the stress space and N_{ijkl} is the tensor of plastic moduli.

The components of both β_{ij} and N_{ijkl} tensors are functions of the plastic strain tensor ϵ_{ij}^P . Thus, Eq. (5.27) describes a yield surface which, in the process of plastic deformation, may increase in size, translate, rotate and change in shape. Preliminary findings indicate that the rule is very promising in properly modeling the behavior of plastically deformed anisotropic soils. Moreover, both strain-hardening and strain-softening can be treated in a single unified way; this is very interesting in connection with overconsolidated clays which, in general, exhibit both hardening and softening characteristics.

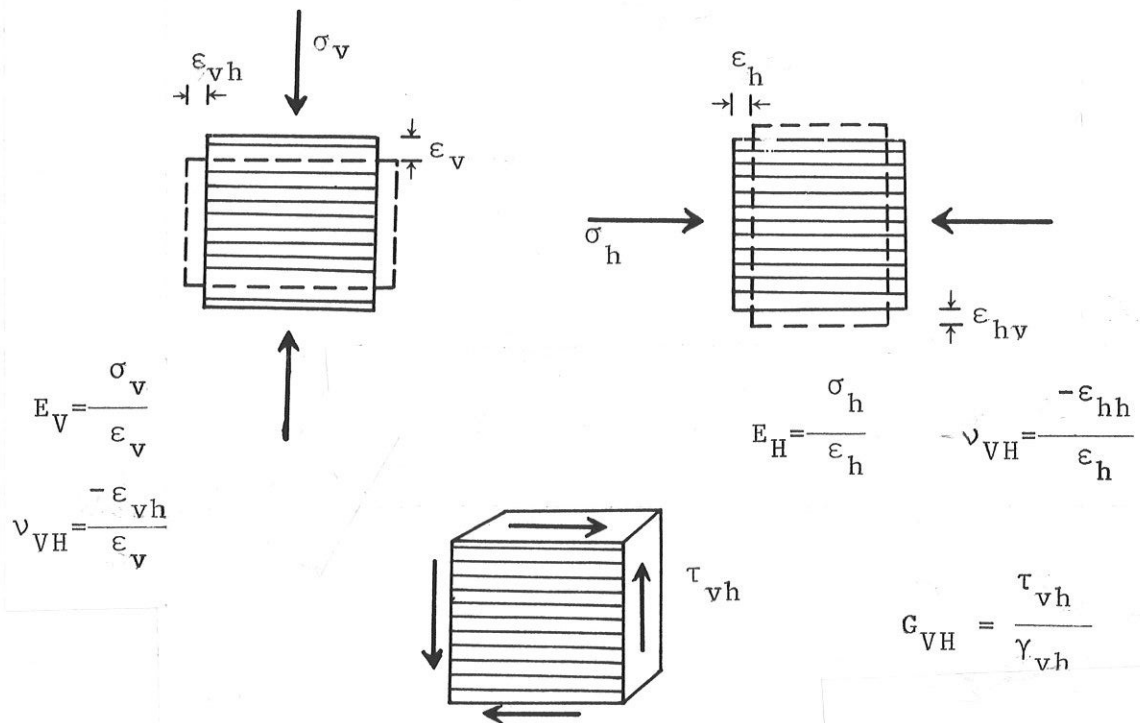


FIG. 5.1 Definition of cross-anisotropic elastic constants

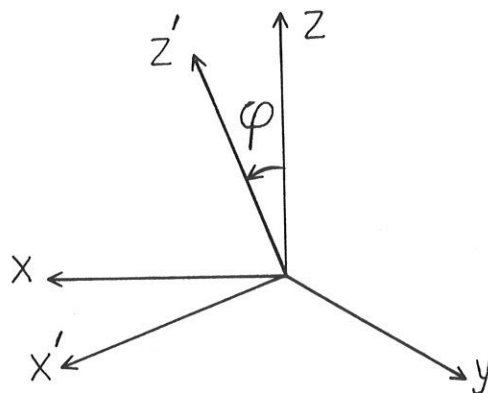


FIG. 5.2 Rotation of co-ordinate system around the y axis

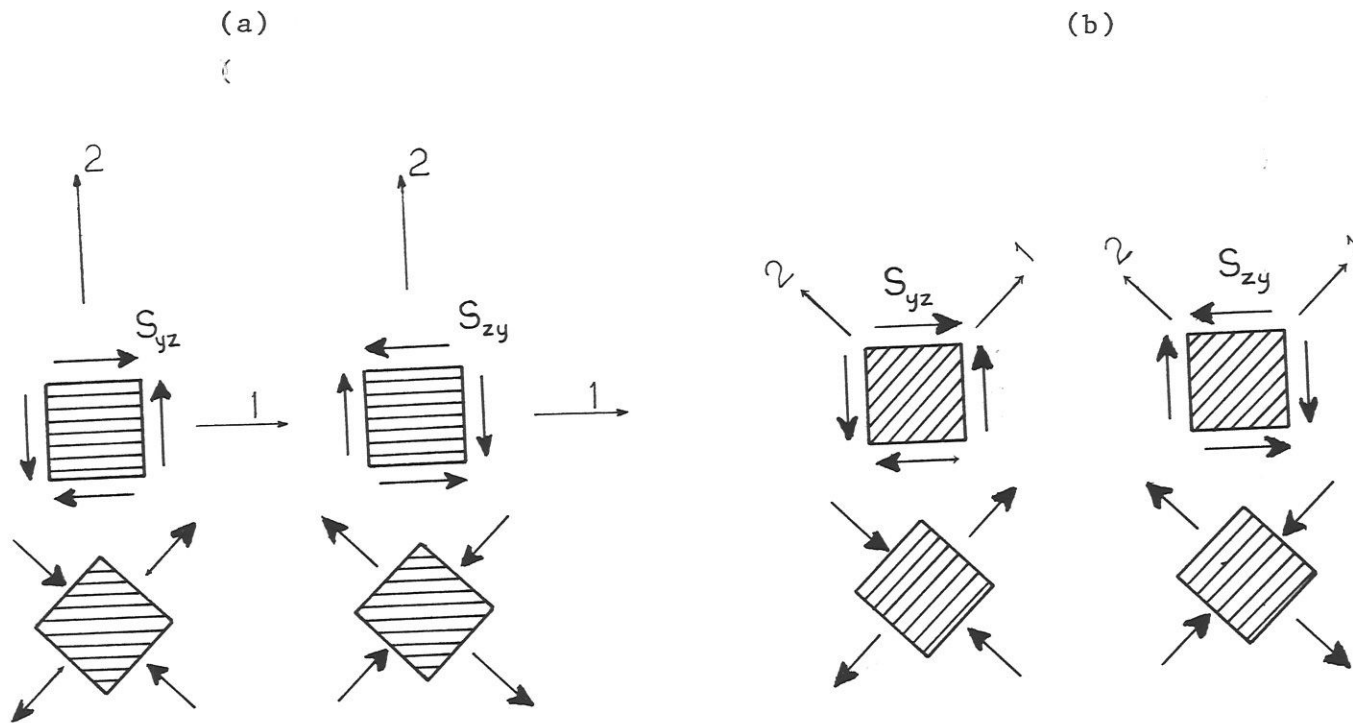


FIG. 5.3 Positive (S_{yz}) and negative (S_{zy}) shear strength of materials behaving differently in compression and extension:
 (a) in principal material directions, $S_{yz} = |S_{zy}|$;
 (b) at 45° to the principal material directions, $S_{yz} \neq |S_{zy}|$

CHAPTER 6

TESTING OF ANISOTROPIC SOILS

Several methods have been developed to determine the anisotropic stress-strain-strength characteristics of soils, both in the laboratory and in-situ. Some of these methods utilize apparatuses that are also used for routine measurements of soil properties while others, apparatuses particularly suitable for , although certainly not restricted to , testing anisotropic soils. The following presentation is not meant to be a detailed state-of-the-art report on the relevant testing procedures, apparatuses and recording devices, but rather an attempt to offer insight into the fundamentals of measuring anisotropic soil parameters and point out some of the special difficulties involved.

6.1 STANDARD TRIAXIAL TESTING

Undrained triaxial tests on solid cylindrical specimens have been used to measure anisotropic soil parameters since the early years of development of the standard triaxial test. Ward and his co-workers (1959, 1965) established the marked deformational anisotropy of the heavily overconsolidated London Clay (see Table 3.2) by testing undisturbed samples prepared so that their axis is vertical, horizontal or inclined at a 45° angle. This method is still in use today (Atkinson, 1975; Mitchell, 1972; Yong & Silvestri, 1979; Gazetas & Botsis, 1981).

The interpretation of such test measurements is rather straightforward. Under undrained conditions there are three independent deformational soil constants, namely E_V , E_H and G_{VH} . The first two can be obtained by testing a vertical and a horizontal sample, respectively. Some difficulty arises in determining G_{VH} , since direct determination from triaxial test data is impossible. A compression test is therefore conducted on a sample with its axis inclined at some angle θ to the vertical, as schematically shown in Fig. 6.1. Such a test allows the Young's modulus E_θ in this direction to be measured. G_{VH} is then computed by utilizing the compliance tensor transformation relations. For an incompressible material ($\nu_{VH} = 1/2$) Eq. 5.15a yields:

$$\frac{1}{E_\theta} = \frac{\cos^4\theta}{E_V} + \frac{\sin^4\theta}{E_H} + \left(\frac{1}{G_{VH}} - \frac{1}{E_V} \right) \sin^2\theta \cos^2\theta \quad (6.1)$$

and if E_V , E_H and E_θ are known, then G_{VH} is found from Eq. (6.1). Gibson recommends the choice of $\theta = 45^\circ$.

The preceding analysis, however, ignores the difficulty in reliably estimating E_θ from triaxial compression tests on inclined specimens. Indeed, as pointed out by Pagano & Halpin (1968) and by Saada (1970), extraneous bending moments and shearing forces are generated at the two ends when an inclined specimen is tested between two rigid and rough platens. Such end effects, whose importance increases with increasing degree of anisotropy, are likely to appreciably influence the computed value of E_θ .

To understand how these end effects are generated, consider a specimen cut at an angle θ to the axis of material symmetry z and subjected to a uniform normal stress $\sigma_{z'} \equiv p$ (Fig. 6.2). The deformation of the specimen with reference to coordinate axes x' , y and z' are obtained by means of Eqs. (5.14) - (5.15):

$$\begin{aligned}
 \epsilon_{x'} &= p S'_{1133} & \epsilon_{x'y} &= p S'_{1233} \\
 \epsilon_y &= p S'_{2233} & \epsilon_{x'z'} &= p S'_{1333} \\
 \epsilon_{z'} &= p S'_{3333} & \epsilon_{yz'} &= p S'_{2333}
 \end{aligned} \tag{6.2}$$

Thus, not only normal but also shear strains are generated due to the non-coincidence of the principal material and imposed-stress axes. Of particular concern is the shear strain $\epsilon_{x'z'}$, governed by the shear coupling compliance S'_{1333} which is obtained from Eq. (5.15). Because of these strains the initially right cylinder deforms into an oblique-angle cylinder, as shown in Fig. 6.2.

However, the end platens of a triaxial apparatus constrain the upper and lower boundaries of the specimen to remain horizontal. As illustrated in Fig. 6.2, the application of uniform vertical end displacements induces

bending moments, which in turn require balancing shearing forces. As a result, a complicated non-uniform state of stress develops in the material and the specimen deforms as shown in the figure. Thus, the measured modulus

$$E_{\theta}^* = \frac{P}{\epsilon_{z'}} \quad (6.3)$$

is not the Young's modulus E_{θ} obtained in a purely uniaxial strain test.

In fact, the ratio

$$\eta = \frac{E_{\theta}}{E_{\theta}^*} \quad (6.4)$$

depends on the material properties, the angle θ , and the length-to-radius ratio of the inclined specimen. A crude estimate of this ratio has been obtained by Pagano & Halpin (1968):

$$\eta \approx 1 - \frac{6 S'_{2333} E_{\theta}}{6 S'_{2323} + \frac{1}{E_{\theta}} \frac{L^2}{R^2}} \quad (6.4a)$$

The compliance parameters S'_{2333} and S'_{2323} are determined according to Eqs. (5.15). It is evident that the error decreases with increasing L/R ratio (slenderness) of the specimen, but without knowing *a priori* the soil constants (especially E_{θ}) it is difficult to assess the size of the error. Therefore, triaxial testing cannot lead to accurate evaluation of the shear modulus G_{VH} . Yet, it is known that G_{VH} may exert a great influence on the distribution of stresses and deformations in anisotropic soils subjected to foundation loading (Gazetas, 1981; Burland et al, 1977). Appendix I presents and evaluates, on the basis of experimental evidence,

a relationship between G_{VH} and the other four independent soil constants. This relation appears to be quite satisfactory for clayey soils and its use, in lieu of the G_{VH} computed from the measured E_{θ} , seems quite reasonable.

Drained triaxial tests. - These tests present the added difficulty of measuring Poisson's ratios ν'_{HH} and ν'_{VH} . Since reliable measurements of lateral strains are not routinely performed during triaxial testing, the theoretical relations between drained and undrained elastic constants proposed by Uriel & Canizo (1971) can be utilized in preliminary computations. Assuming cross-anisotropic soil skeleton and incompressibility of the fully saturated soil, these relations are:

$$n = \frac{E_H}{E_V} = \frac{2(n' - n'\nu'_{HH} - 2\nu'_{HV})^2}{(2+n'-4\nu'_{HV}-2\nu'_{HH}) - (1-\nu'_{HH}-\nu'_{HV})^2} \quad (6.5a)$$

$$\frac{E_H}{E'_H} = \frac{2 + n' - 4\nu'_{HV} - 2\nu'_{HH}}{(2+n'-4\nu'_{HV}-2\nu'_{HH}) - (1-\nu'_{HH}-\nu'_{HV})^2} \quad (6.5b)$$

$$n' = E'_H/E'_V \quad (6.5c)$$

where the prime denotes effective-stress (drained) parameters. Thus, after measuring E'_H and E'_V from drained tests on horizontal and vertical specimens, Eqs. (6.5) can be used to solve for ν'_{HH} and ν'_{HV} , if the undrained moduli E_H and E_V are known. The reader is cautioned, however, that no experimental verification of Eq. (6.5) has been documented.

6.2 RESONANT COLUMN TESTS

Resonant-column tests are particularly well suited for measuring Young's and shear moduli at low levels of strain. Either compression or shear waves are propagated through solid or hollow cylindrical specimens. The exciting frequency is adjusted until the specimen resonates. The appropriate modulus is then computed from the resonant frequency and the geometric properties of the specimen and the driving apparatus (Woods, 1978).

Young's moduli E_H and E_V are determined from the resonant frequencies of horizontal and vertical specimens subjected to longitudinal waves. It is usually assumed that such waves propagate at velocities $C_H = \sqrt{E_H/\rho}$ and $C_V = \sqrt{E_V/\rho}$. This, however, is only approximately true when the wavelengths involved are very large compared with the radius of the specimen. In general, due to Poisson's effect, secondary lateral vibrations may also take place and influence the "effective" velocity. A better estimate is obtained by multiplying the above values of C_H and C_V by a correction factor

$$\delta = 1 - \nu \pi^2 \left(\frac{R}{\Lambda_r} \right)^2 \quad (6.6)$$

where: R = the radius of the cylinder; $\Lambda_r = C/f_r$; and f_r = the resonant frequency (in cps). For vertical samples the Poisson's ratio ν is equal to ν_{VH} , but for horizontal samples Poisson's ratio varies from ν_{HV} to ν_{HH} . A reasonable approximation is to take $\nu = (\nu_{HV} + \nu_{HH})/2$.

The shear modulus G_{VH} can be directly obtained from the resonant frequency of a vertical specimen subjected to torsional oscillation. The

velocity of the resulting shear waves is $C_s = \sqrt{G_{VH}/\rho}$. No secondary waves are propagated and, therefore, G_{VH} is directly and reliably evaluated by this procedure.

6.3 TRUE TRIAXIAL TESTING ON PRISMATIC SPECIMENS

Numerous true triaxial devices have been developed in recent years to overcome the limitations of the standard cylindrical triaxial testing. They use prismatic specimens of cubic or parallelepiped shape and allow three principal stresses to be independently applied by means of three pairs of rigid platens or flexible membranes or a combination of the two.

These apparatuses are very well suited for studying inherent as well as induced anisotropy of sands and clays, since they allow any direction of deposition relative to the applied principal stress directions. Moreover, the range of stress paths that can be imposed on a specimen is much larger than in the conventional triaxial cells.

Several investigators have used true triaxial cells to study the anisotropy of artificially prepared sands (Arthur & Menzies, 1972; Tatsuoka, 1976; Yamada & Ishihara, 1979) or natural clays (Yong & Silvestri, 1979). It is noted, however, that these studies cannot directly lead to an evaluation of the shear modulus G_{VH} .

Moreover, most of these devices are mechanically complex and require special care in preparation and placement of the specimen. Non-uniform states of stress are generated if the load is applied via rigid platens; and the relatively short distances of the center of the specimen from such

boundaries do not allow the beneficial Saint Venant effect to take place.

Saada et al (1980) has presented a chronological development of the true triaxial testing devices with a discussion of their advantages and limitations.

6.4 HOLLOW CYLINDER UNDER AXIAL AND TORSIONAL STRESSES

The idea of subjecting thin and long hollow cylindrical specimens to combined axial and torsional stresses offers perhaps the most rational (from a mechanics point of view) method to evaluate the anisotropic stress-strain-strength characteristics of soils and to study the effects of rotation of the principal stress axes on various soil parameters. This idea, apparently being first introduced in the 1930's, has been extensively utilized in the Soil Mechanics Laboratory of Case Institute of Technology by Saada & his co-workers since 1965 (Saada, 1967; 1970; Saada & Ou, 1973; Saada & Bianchini, 1975). The reader is referred to these publications for more detailed information.

To avoid all extraneous bending and shear end effects that develop when inclined specimens are tested in axial compression or extension, the specimens are kept vertical, while the inclination of the principal stresses may be arbitrary. To perform meaningful strain measurements, the inclination of principal stresses is kept constant. The principal strains, however, assume a different direction depending on the anisotropy of the soil, the magnitude of the applied stresses and, of course, the inclination of these stresses relative to the principal axes of material symmetry. This is achieved by keeping the ratio of axial to torsional stresses constant during a test. As indicated in Fig. 6.3, the direction of the major

principal stress in a thin and long hollow cylinder initially consolidated under the same inner and outer cell pressure and then subjected to additional axial and torsional loading is given by the angle θ :

$$\theta = \frac{1}{2} \arctan \frac{2 \tau_{\theta z}}{\sigma_z} \quad (6.7)$$

Thus, θ remains constant if $\tau_{\theta z}/\sigma_z$ is kept constant. By changing the value of this ratio an unlimited number of inclinations can be investigated.

It is noted, however, that the intermediate principal stress is always acting in the radial direction, $\sigma_2 = \sigma_r$, and is always equal to σ_θ (both are equal to the cell pressure). It is also fair to say that preparation of thin hollow cylinder specimens is more complicated than that of standard triaxial testing. Also sample disturbance is certainly greater with hollow than with solid specimens.

6.5 IN-SITU MEASUREMENTS

In principle, many field techniques that are currently employed to evaluate deformational soil parameters in-situ (such as seismic cross-hole, up-hole or down-hole surveys, surface wave techniques, torsional or shear footing vibration methods, etc.) can be adapted to yield information regarding anisotropic soil properties. For example, by generating vertically or horizontally polarized shear waves from a seismic source in a borehole, one may be able to estimate G_{VH} or G_{HH} , respectively. Hoar & Stokoe (1977) have described such a source consisting of a torque rod

and torque foot and placed near the bottom of a borehole. Using the torque foot with a torsion impulse, horizontally polarized shear waves (SH-waves) are generated, while using an open pipe with a vertical impact, vertically polarized shear waves (SV-waves) are generated in the soil.

Apparently, however, such techniques have not yet been fully exploited to study deformational soil anisotropy in-situ.

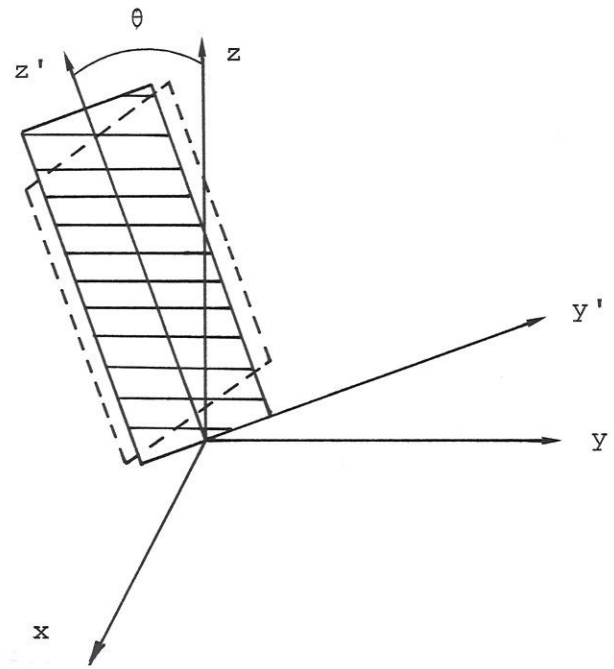
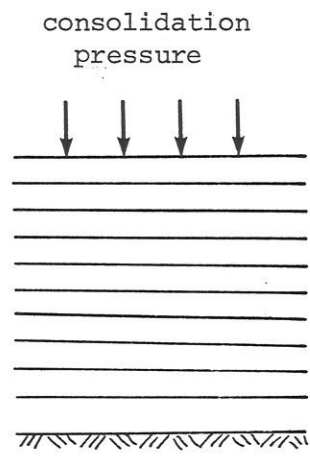


FIG. 6.1 Geometry of inclined specimen and co-ordinate axes

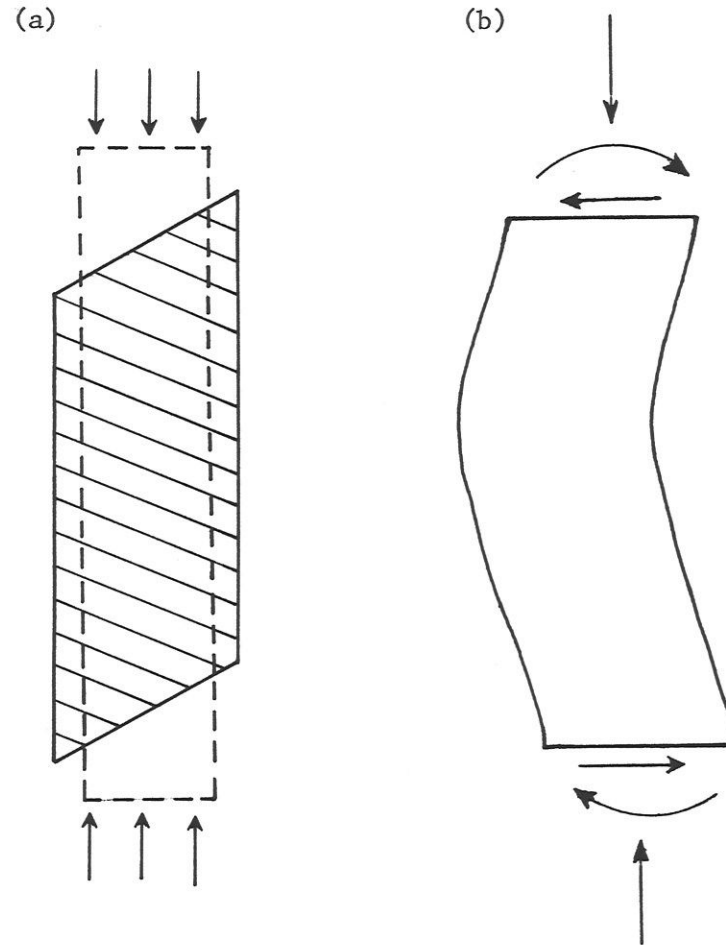


FIG. 6.2 (a) Deformation into an oblique-angle cylinder of a specimen subjected into a uniform axial state of stress
(b) Bending moments and shear forces are created at the rough rigid platens of a standard triaxial apparatus

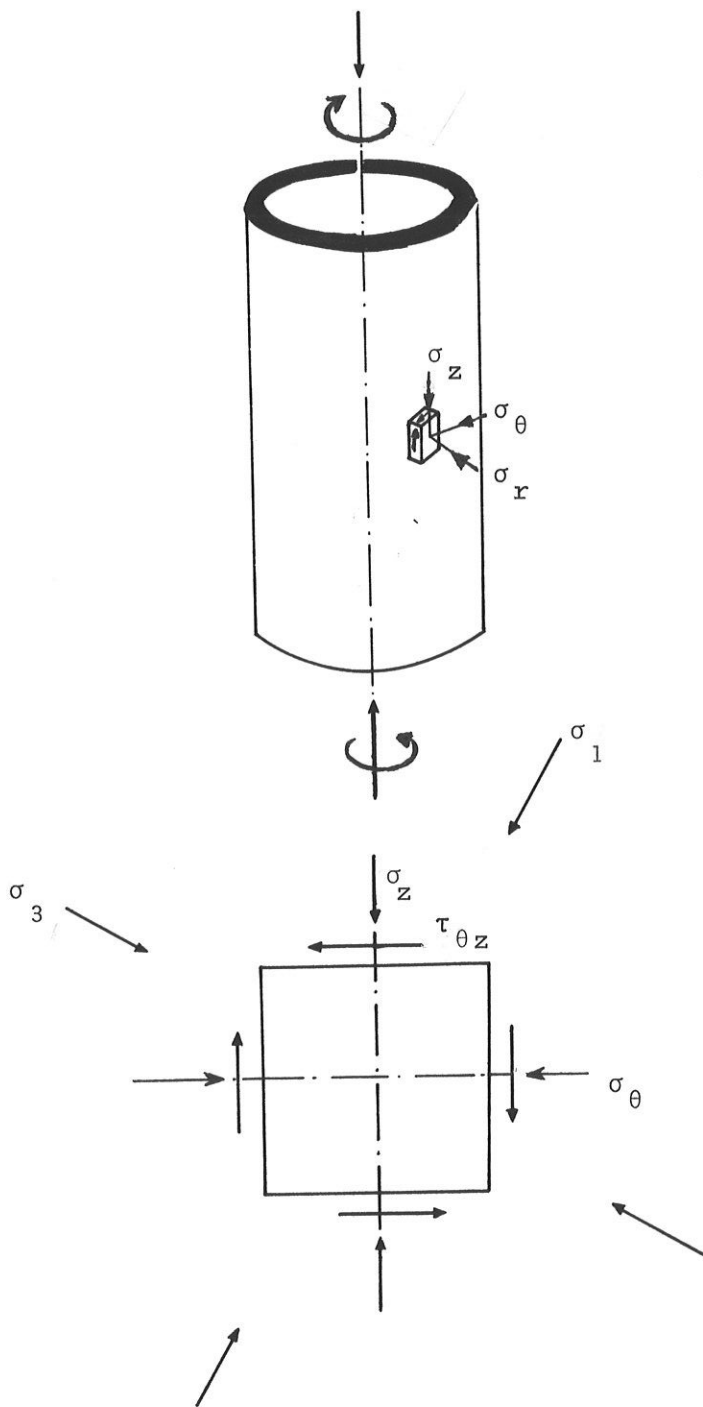


FIG. 6.3 State of stress in a hollow cylindrical sample subjected to axial and torsional loading.

REFERENCES

1. Aas, G. (1965). A study of the effect of vane shape and rate of strain on the measured values of in-situ shear strength of clays. Proc. 6th Int. Conf. Soil Mech. Fdn. Engrg., Montreal, 141.
2. Arthur, J.R.F. and Menzies, B.K., (1972). Inherent anisotropy in a sand. Geotechnique, 22, 1, 115-128.
3. Arthur, J.R.F. and Phillips, B.K., (1975). Homogeneous and layered sand in triaxial compression. Geotechnique, 25, 2, 799-815.
4. Atkinson, J.H. (1975). Anisotropic elastic deformations in laboratory tests on undisturbed London Clay. Geotechnique, 25, 2, 357-374.
5. Baltov, A. and Sawczuk, A., (1965). A rule of anisotropic hardening. Acta Mechanica, 1, 2, 81-92.
6. Barden, L. (1971). Examples of clay structure and its influence on engineering behavior Proc. Roscoe Mem. Symp. Cambridge Univ., 195-205.
7. Barden, L. (1972). Influence of structure on deformation and failure in clay soil. Geotechnique 22, 159-163.
8. Bazant, Z.P., Ozaydin, I.K. and Krizek, R.J. (1975). Micromechanics model for creep of anisotropic clay. Jnl. Engrg. Mech. Div. ASCE, 101, EM1, 57-78.
9. Bhaskaran, R. (1975). Variability in strength and deformation characteristics of anisotropic clays. Symp. Recent Development Analysis Soil Behaviour and Application to Geotechnical Structures, Univ. of N.S.W., Sydney, Australia, 289.
10. Bishop, A.W., Webb, D.L., and Lewin, P.I. (1965). Undisturbed samples of London Clay from the Ashford Common Shaft: Strength-effective stress relationships. Geotechnique, 15, 1, 1-31.
11. Botsis, J. and Gazetas, G. (1981). A new anisotropic hardening/softening plasticity model. Res. Rep. 8103, Case Western Reserve Univ.
12. Brekhovskikh, L.M. (1960). Waves in layered media. Academic Press, New York.
13. Brooker, E.W., Ireland, H.O. (1965). Earth pressure at rest related to stress history. Canadian Geotech. Jnl, 2, 1-15.
14. Burland, J.B., Broms, B.B. and Demello, V.F.B. (1977). Behavior of foundations and structures. Proc. IX Int. Conf. Soil Mech. & Fdn. Engrg, Tokyo, 495-546.
15. Casagrande, A. & Carillo, N. (1944). Shear failure of anisotropic materials. Proc. Boston Soc. Civ. Engrs, 31, 74-87.

15. Cummings, A.E. (1935). Distribution of stress under a foundation. Proc. ASCE, 61, p. 823.
16. Davis, E.H. and Christian, J.T., (1971). Bearing capacity of anisotropic cohesive soils. Proc. ASCE, 97, SM5, 753-769.
17. Davis, E.H. and Deresiewicz, H., (1977). A discrete probabilistic model for mechanical response of a granular medium. Acta Mechanica, 27, 69-89.
18. DeJosselin de Jong, G., (1971). The double sliding, free rotating model for granular assemblies. Geotechnique, 21, 155-163.
19. Duncan, J.M. and Seed, H.B., (1966). Anisotropy and stress orientation in clay. Proc. ASCE, 92, SM5, 21-50.
20. El-Sohby, M.A. and Andrawes, K.Z. (1973). Experimental examination of sand anisotropy, Proc. 8th Inter. Conf. Soil Mech. Found. Engng, 1.1, 103.
21. Fookes, P.G. and Denness, B., (1969). Fissure patterns in the creaceous sediments, Geotechnique, 19, 4, 453-477.
22. Franklin, A.G. and Mattson, P.A., (1972). Directional variation of elastic wave velocities in oriented clay. Clay and clay min. 20 285-293.
23. Gazetas, G. (1981). Strip foundations on cross-anisotropic layered soil subjected to static and dynamic loading. Geotechnique, 31, No. 2.
24. Gazetas, G. (1981). Stresses and displacements in cross-anisotropic soils. J. Geotech. Engrg. Div., ASCE.
25. Gazetas, G. and Botsis, J. (1981). Stress-strain-strength behavior of overconsolidated kaolinite. Res. Rep. 8104, Case Western Reserve University.
26. Gerrard, C.M. (1977). Background to mathematical modelling geomechanics: The roles of fabric and stress history. Fin. Elem. in Geomech. G. Gudelus (ed.), J. Wiley, N. York, 33-120.
27. Gerrard, C.M. and Willoughby, D.R. (1968). Deformation of sand in hydrostatic compression, Journal of the soil mechanics Division, ASCE.
28. Gerrard, C.M. and Harrison, W.J. (1972). Effect of inclined planar fabric features on behavior of loaded rock mass. Proc. 2nd Cong. Int. Soc. Rock. Mech., Belgrade, Yugoslavia, 2-20.
29. Gibson, R.E. (1974). The analytical method in soil mechanics. Geotechnique 24, No. 2, 115-140.
30. Gilkes, R.J. (1968). Clay mineral provinces in the tertiary sediments of the Hampshire basin clay, Minerals, 7, 351-361.

31. Gol'denblat, I.I., and Kopnov, V.A. (1968). Criteria of strength and plasticity of construction materials. (in Russian). Mashinostroenie, Moscow, U.S.S.R.
32. Gol'denblat, I.I., & Kopnov, V.A. (1971). General theory of criteria of strength for isotropic and anisotropic materials. Problemy Prochnosti, Moscow, U.S.S.R., No. 2 (translation), 65-69.
33. Graton, L.C. and Fraser, H.J. (1935). Systematic packing of spheres with particular relation to porosity and permeability, *J. of Geology*, 43, 785-909.
34. Hansen, J.B. and Gibson, R.E. (1949). Undrained shear strengths of anisotropically consolidated clays. *Geotechnique*, 1, 189-204.
35. Harrison, W.J. and Gerrard, C.M. (1972). Elastic theory applied to reinforced earth. *Proc. ASCE*, 98, SML2, 1325-1345.
36. Hearmon, R.F.S. (1961). An introduction to applied anisotropic elasticity. Oxford Univ. Press.
37. Hill, R. (1950). The mathematical theory of plasticity. Oxford Univ. Press.
38. Hoar, R.J. and Stokoe, K.H. (1977). Generation and measurement of shear waves in-situ. ASTM Symposium, Denver.
39. Jaeger and Cook (1976). Fundamentals of rock mechanics. Methuen Co.
40. Kallstenius, T. and Bergau, W. (1961). Research on the texture of granular masses, *Proc. Fifth Inter. Conf. Soil Mech. Found. Engng*, 1, 158-165.
41. Kirkpatrick, W.M. and Rennie, I.A. (1973). Clay structure in laboratory prepared samples, *Proc. Inter. Symp. Soil Structure, Gothenburg, Swedish Geotech. Soc.* 103-111.
42. Kolbuszewski, J. and Jones, R.H. (1961). The preparation of sand samples for laboratory testing. *Proc. Midland SMFE Soc.*, 4, 107-123.
43. Lade, P.V. (1972). The stress-strain and strength characteristics of cohesionless soils. Ph.D. Thesis, U. Calif. Berkeley.
44. Ladd, C.L. et. al (1977). Stress-deformation and strength characteristics. IX Int. Conf. Soil Mech. Fdn. Engrg., Tokyo, 421-494.
45. Lafeber, D. and Willoughby, D.R. (1971). Fabric symmetry and mechanical anisotropy in natural soils, *Proc. Aust.-New Zealand Conf. Geomech.*, Melbourne, 1, 165-174.
46. Lafeber, D. and Willoughby, D.R. (1970). Morphological and mechanical anisotropy of a recent beach sand, *Proc. of Symp. on Foundations on Interbedded Sands, CSIRO, Perth*, 1, 80-86.

47. Lambe, T.W. (1958). The structure of compacted clay. *Journal of the Soil Mechanics and Foundations Division A.S.C.E.*, 84, No. SM2, 34.
48. LaRochelle, P. and Lefebvre, G. (1971). Sampling and disturbance in Champlain clays. ASTM Publ. No. 483, 143-163.
49. Lekhnitskii, S.G. (1973). Theory of elasticity of an anisotropic elastic body. Holden-Day Inc. San Francisco, CA.
50. Livneh, M. and Greenstein, J. (1974). Plastic equilibrium in anisotropic cohesive clays. *Soils and Foundations*, 14, 1-11.
51. Lo, K.Y. (1965). Stability of slopes in anisotropic soils. *Jnl. Soil Mech. Fdns. Div. A.S.C.E.*, 91, SM4, 85-106.
52. Mahmood, A. (1973). Fabric-mechanical property relationships in fine granular soils. Ph.D. dissertation, University of California, Berkeley.
53. Mahmood, A. and Mitchell, J.K. (1974). Fabric-property relationships in fine granular materials. *Clays and Clay Minerals*, 22, No. 5/6, 397-408.
54. Martin, R.T. and Ladd, C.C. (1970). Fabric of consolidated kaolinite. M.I.T. Report, R70-15.
55. Martin, R.T. (1966). Quantitative fabric of wet kaolinite. Fourteenth National Clay Conference, 271-287.
56. Mehrabadi, M.M., Nemat-Nasser, S. and Oda, M. (1980). On statistical description of stress and fabric in granular materials. Rept. No. 80-4-29. Northwestern University.
57. Mitchell, R.J. (1970). On the yielding and mechanical strength of Leda clays. *Canad. Geotech. J.*, 7, 297-312.
58. Mitchell, R.J. (1972). Some deviations from isotropy in a lightly over-consolidated clay, *Geotechnique*, 22, 459-467.
59. Mitchell, J.K. (1976). Fundamentals of soil behavior. J.Wiley & Sons, Inc.
60. Morland, L.W. (1976). Elastic anisotropy of regularly jointed media. *Rock Mechanics*, 8, 35-48.
61. Oda, M. (1972a). Initial fabrics and their relations to mechanical properties of granular material. *Soil Fdn* 12, No. 1, 17-36.
62. Oda, M. (1972b). The mechanism of fabric changes during compressional deformation of sand. *Soil Fdn*. 12, No. 2, 1-18.
63. Pagano, N.J. and Halpin, J.C. (1968). Influence of end constraint in the testing of anisotropic bodies. *Jul. Compos. Mat.* 2, 1, 18-31.
64. Parkin, A.K., Gerrard, C.M. and Willoughby, D.R. (1968). Discussion on deformation of sand in shear, *J. Soil Mech. and Found. Div., ASCE*, 94, SM1, 336-340.

65. Parry, R.H.G. and Nadarajah, V. (1974). Anisotropy in a natural soft clayey silt , *Engineering Geology*, 8, 287-309.
66. Pickering, D.J. (1970). Anisotropic elastic parameters for soil. *Geotechnique* 20, 3, 271-276.
67. Quigley, R.M., and Thompson, C.D. (1966). The fabric of anisotropically consolidated sensitive marine clay. *Canadian Geotechnical Jnl*, Vol. III, No. 2, 61-73.
68. Rowe, P.W. (1972). The relevance of soil fabric to site investigation practice , *Geotechnique*, 22, 2, 195-300.
69. Rowe, P.W. (1962). The stress-dilatancy relation for static equilibrium of an assembly of particles in contact , *Proc. Roy. Soc. A.*, 269, 500-527.
70. Saada, A.S. and Ou, C. (1973). Strain-stress relations and failure of anisotropic clays , *J. Soil Mech. Fnds. Div., ASCE*, 99, No. SM12, 1091-1111.
71. Saada, A.S. (1970). One dimensional consolidation in triaxial cell. *Jnl. Soil Mech. and Fdn Div. ASCE*, 96, No. SM3, 1085-1087.
72. Saada, A.S. (1967). Stress-controlled apparatus for triaxial testing. *Jnl. Soil Mech. and Fdn Div. ASCE*, 93 , No.SM6, 61-77.
73. Saada, A.S. and Bianchini, G.F. (1975). Strength of 1-Dimensionally consolidated clays. *Proc. ASCE*, 101, GT11, 1151-1168.
74. Saada, A.S. et. al (1980). Strength laboratory testing of soils: a state of the art. *ASTM symposium, Chicago, June 25*.
75. Salamon, M.D.G. (1968). Elastic moduli for a stratified rock mass. *Int. Jnl. Rock Mech. Min. Sci.*, 5, 519-527.
76. Simons, N.E. (1971). The stress path method of settlement analysis applied to London clay , *Proc. Roscoe Memorial Symp. Cambridge Univ.*, 241-252.
77. Skempton, A.W. and Henkel, D.J. (1975). Tests on London clay from deep borings at Paddington, Victoria and the South Bank , *Proc. Fourth Int. Conf. Soil Mech. and Found. Eng., London*, 1, 100-106.
78. Skempton, A.W. and Hutchinson, J. (1969). Stability of natural stopes and embankment foundations , *Proc. Seventh Inter. Conf. Soil Mech. and Found. Engng, Mexico*, (state-of-art, Volume, 291-340).
79. Soderman, L.G. and Quigley, R.M. (1965). Geotechnical properties of three Ontario clays. *Canad. Geotech. Jnl*, 2, 167-189.
80. Spencer, A. J.M. (1964). A theory of the kinematics of ideal soils under plane strain conditions. *Jnl. Mech. Phys. Solids*, 12, 337-351.

81. Tatsuoka, F. (1976). Stress-dilatancy relations of anisotropic sands in three dimensional stress condition. *Soils and Foundations*, 14, No. 3, 51-65.
82. Tsai, S.W. and Wu, E.M. (1971). A general theory of strength for anisotropic materials. *Jnl. Compos. Mater.* 5, 58-80.
83. Uriel, A.O. and Canizo, L. (1971). On the elastic anisotropy of soil. *Geotechnique*, 21, No. 3, 262-267.
84. U.S. Army Corps of Engineers, Waterway Exp. Station (1954). Investigations of pressures and deflections for flexible pavements. Rpt No. 4, Homog. sand test section. Tech. Memo No. 3, 323.
85. Vidal, H. (1969). The principle of reinforced earth. *Highway Res. Rec.*, 282.
86. Ward, W.H., Marsland, A., and Samuels, S.G. (1965). Properties of the London clay at the Ashford Common Shaft, *Geotechnique*, 15, 4, 321-344.
87. Ward, W.H. Samuels, S.G. and Butler, M.E. (1959). Further studies of the properties of London clay, *Geotechnique* 9, 33-58.
88. Wardle, L.J. and Gerrard, (1972). The "equivalent" properties of layered rock and soil masses. *Int. J. of Rock Mech.*, Wien, 4, 155-175.
89. Wu, E.M. (1974). Phenomenological anisotropic failure criterion. *Composite materials*, Chap. 9, (ed. G.P. Sendekyj) 353-431.
90. Woods, R.D. (1978). Measurement of dynamic soil properties, state of the art. Proc. ASCE Specialty Conf. on Earthq. Engng and Soil Dyn., Pasadena.
91. Yamada, Y. and Ishihara, K. (1979). Anisotropic deformation characteristics of sand under three dimensional stress conditions. *Soils & Foundations*, 19, 2, 79-94.
92. Yamanouchi, T. (1970). Experimental study on the improvement of the bearing capacity of soft ground by laying a resinous net. Symp. Fdn. on Interbedded Sands, CSIRO, Australia.
93. Yong, R.N. (1971). Yielding and failure of a clay under triaxial stresses. *Jnl. Soil Mech. Fdn. Engrg. Div. ASCE*, 97, 1, 159-176.
94. Yong, R.N. and Silvestri, V. (1979). Anisotropic behavior of a sensitive clay. *Canadian Geot. J.* 16, 335-350.

APPENDIX

For many types of soils the following relationship has been found to approximately hold between shear modulus G_{VH} and the other elastic constants:

$$G_{VH} = \frac{D_{11}D_{33} - D_{13}^2}{D_{11} + 2D_{13} + D_{33}} \quad (A1)$$

in which

$$\begin{aligned} D_{11} &= \frac{E_H}{a} (1 - n v_{VH}^2) \\ D_{12} &= \frac{E_H}{a} (n v_{VH}^2 + v_{HH}) \\ D_{13} &= \frac{E_H}{a} v_{VH} (1 + v_{HH}) \\ D_{33} &= \frac{E_V}{a} (1 - v_{HH}^2) \end{aligned} \quad (A2)$$

$$a = (1 + v_{HH}) (1 - v_{HH}^2 - 2n v_{VH}^2)$$

For an isotropic material: $v_{VH} = v_{HH} \equiv v$ and $E_V = E_H \equiv E$ and Eq. A1 reduces to the well known relation between moduli and Poisson's ratio of isotropic media:

$$2G_{VH} \equiv 2G = E/(1+v) \quad (A3)$$

Moreover, for an incompressible material Eq. A1 simplifies to

$$\frac{G_{VH}}{E_V} = \frac{1}{4-n} \quad (A3)$$

The validity of Eq. A1 has been verified by means of numerous published experimental data which are summarized in Table A1 on the next page. Using the reported values of n , ν_{VH} , ν_{HH} and E_V , shear moduli were computed from Eq. A1 or Eq. A3 (whichever was appropriate); these moduli are also depicted in the Table for comparison with the experimental values.

The performance of Eq. A1 (or A3) appears to be quite satisfactory and thus, it is recommended that it be used for estimating the shear modulus of anisotropic soils, whenever appropriate experimental measurements are not available.

TABLE A1

clays and evaluation

Description of Soil	Reference	Measured values				Computed (Eqn 6) G_{VH}/E_V
		n	ν_{VH}	ν_{HH}	G_{VH}/E_V	
HEAVILY OVERCONSOLIDATED LONDON CLAY (Ashford) (Undrained loading)	Ward et al. (1959)					
1. Depth - 30 ft	Ward et al. (1965)	1.35	0.50	0.325	0.35 ⁽¹⁾	0.355
2. Depth - 50 ft	Gibson (1974)	1.59	0.50	0.205	0.37 ⁽¹⁾	0.41
3. average of all samples		1.80	0.50	0.08	0.38 ⁽¹⁾	0.46
HEAVILY OVERCONSOLIDATED LONDON CLAY (Barbican Arts Centre). (Drained Loading)	Atkinson (1975)	2.00	0.19	0.00	0.536 ⁽²⁾	0.553
LIGHTLY OVERCONSOLIDATED KAOLINITE CLAY (Florida Edgar Plastic Kaolin). (Undrained Loading)	Saada et al. (1978)					
1. $\sigma'_c = 40$ psi, water content = 40.7%		1.25	0.50	0.375	0.356	0.364
2. $\sigma'_c = 60$ psi, water content = 38.7%		1.355	0.50	0.322	0.362	0.378
NORMALLY CONSOLIDATED ILLITE CLAY (Grundite) (Undrained Loading)	Bianchini (1980)					
1. $\sigma'_c = 70$ psi, w = 29.5%		1.17	0.50	0.415	0.355	0.353
2. $\sigma'_c = 60$ psi, w = 38.1%		1.13	0.50	0.436	0.322	0.310
COLORADO CLAY SHALE (Drained Loading)	Kaarsberg (1968)	1.38	0.197	0.266	0.423	0.524
SENSITIVE, NATURALLY CEMENTED CHAMPLAIN SEA CLAY (Canada). (Drained Loading)	Yong et al. (1979)	0.62	0.35	0.20	0.205 ⁽¹⁾	0.187

(1) Estimated from E_{450} using equation (21) of Gibson, 1974.

(2) Estimated by the Author from undrained tests on the basis of the theoretical formulas of Uriel & Kanizo (1971), as explained in Appendix A,